

The Method of Fundamental Solutions for Inverse Problems Associated with the Steady-State Heat Conduction in the Presence of Sources

Liviu Marin¹

Abstract: The application of the method of fundamental solutions (MFS) to inverse boundary value problems associated with the steady-state heat conduction in isotropic media in the presence of sources, i.e. the Poisson equation, is investigated in this paper. Based on the approach of Alves and Chen (2005), these problems are solved in two steps, namely by finding first an approximate particular solution of the Poisson equation and then the numerical solution of the resulting inverse boundary value problem for the Laplace equation. The resulting MFS discretised system of equations is ill-conditioned and hence it is solved by employing the singular value decomposition (SVD), whilst the choice of the optimal truncation number, which is the regularization parameter in this case, is based on the L-curve criterion. Three examples in smooth and piecewise smooth, simply and doubly connected, two-dimensional domains are considered and the convergence and stability of the proposed numerical method are analysed, based on the numerical experiments undertaken.

Keyword: Meshless method, method of fundamental solutions, steady-state heat conduction, inverse problem, regularization, singular value decomposition.

1 Introduction

The method of fundamental solutions (MFS) was originally introduced by Kupradze and Aleksidze (1964), whilst its numerical formulation was first given by Mathon and Johnston (1977). The main idea in the MFS consists of approximating the solution of the problem by a linear com-

ination of fundamental solutions with respect to some singularities/source points which are located outside the domain. Then the original problem is reduced to determining the unknown coefficients of the fundamental solutions and the coordinates of the source points by requiring the approximation to satisfy the boundary conditions and hence solving a nonlinear problem. If the source points are fixed *a priori* then the coefficients of the MFS approximation are determined by solving a linear problem. An excellent survey of the MFS and related methods over the past three decades has been presented by Fairweather and Karageorghis (1998).

The advantages of the MFS over domain discretisation methods, such as the finite-difference (FDM) and the finite element methods (FEM), are very well documented, see e.g. Fairweather and Karageorghis (1998). In addition, the MFS has all the advantages of boundary methods, such as the boundary element method (BEM), as well as several advantages over other boundary methods. For example, the MFS does not require an elaborate discretisation of the boundary, integrations over the boundary are avoided, the solution in the interior of the domain is evaluated without extra quadratures, its implementation is very easy and only little data preparation is required. The most arguable issue regarding the MFS is still the location of the source points. However, this problem can be overcome by employing a nonlinear least-squares minimisation procedure, see Fairweather and Karageorghis (1998). Alternatively, the source points can be prescribed *a priori*, see Balakrishnan and Ramachandran (1999), and Golberg and Chen (1996), and the post-processing analysis of the errors can indicate their optimal location.

The MFS has been successfully applied to solving

¹Institute of Solid Mechanics, Romanian Academy, 15 Constantin Mille, Sector 1, PO Box 1-863, RO-010141 Bucharest, Romania. E-mail: marin.liviu@gmail.com

a wide variety of boundary value problems. Karageorghis and Fairweather (1987) have solved numerically the biharmonic equation using the MFS and later their method has been modified in order to take into account the presence of boundary singularities in both the Laplace and the biharmonic equations by Poulikkas, Karageorghis and Georgiou (1998a). Furthermore, Poulikkas, Karageorghis and Georgiou (1998b) have investigated the numerical solution of the inhomogeneous harmonic and biharmonic equations by reducing these problems to the homogeneous corresponding cases and subtracting a particular solution of the governing equation. The MFS has been formulated for three-dimensional Signorini boundary value problems and it has been tested on a three-dimensional electropainting problem related to the coating of vehicle roofs in Poulikkas, Karageorghis and Georgiou (2001). Karageorghis and Fairweather (2000) have studied the use of the MFS for the approximate solution of three-dimensional isotropic materials with axisymmetrical geometry and both axisymmetrical and arbitrary boundary conditions. The application of the MFS to two-dimensional problems of steady-state heat conduction and elastostatics in isotropic and anisotropic bimetals has been addressed by Berger and Karageorghis (1999; 2001), whilst Poulikkas, Karageorghis and Georgiou (2002) have successfully applied the MFS for solving three-dimensional elastostatics problems. The MFS, in conjunction with the singular value decomposition (SVD), has been employed by Ramachandran (2002) in order to obtain numerical solutions of the Laplace and the Helmholtz equations.

The steady-state heat conduction in isotropic media in the presence of heat sources is modelled by the Poisson equation, see e.g. Kraus, Aziz and Welty (2001), and Beck, Blackwell and St. Clair (1985). However, in many important applications the boundary conditions may not be completely known due to technical difficulties associated with the data acquisition. For example, a part of the boundary is inaccessible to direct measurements, as in the case of the re-entry of a vehicle from atmosphere, and the presence of mea-

suring devices, such as thermocouples, will disturb the physical process under investigation and hence only inaccurate data can be collected. Additional data may be supplied in the form of either other type of boundary conditions on the same accessible part of the boundary or measurements are taken at some internal points in the solution domain. These are examples of inverse problems, including the Cauchy problem as a particular case, and it is well-known that they are generally ill-posed, i.e. the existence, uniqueness and stability of their solutions are not always guaranteed, see e.g. Hadamard (1923).

It is important to mention that over the last two decades, various numerical methods have been employed to solve inverse problems that occur in several branches of engineering and sciences, such as steady state heat conduction [Lesnic, Elliott and Ingham (1997; 1998), Ling and Atluri (2006), Liu (2006), Liu, Liu and Hong (2007)], fluid flow [Zeb, Ingham, Elliott and Lesnic (2000; 2002)], rock mechanics [Mustata, Harris, Elliott, Lesnic and Ingham (2000), Harris, Mustata, Elliott, Ingham and Lesnic (2008)], elasticity [Chao, Chen and Lin (2001), Marin, Elliott, Ingham and Lesnic (2001; 2002)], electrochemical processes [Noroozi, Sewell and Vinney (2006)], automatic inverse problem engine [de Lacerda and da Silva (2006)] computerised tomography [Mera, Elliott and Ingham (2006), Shiozawa, Kubo, Sakagami and Takagi (2006)], vibrations [Huang and Shih (2007)], electromagnetism [Marin, Power, Bowtell, Sanchez, Becker, Glover and Jones (2008)], etc.

Several BEM-based algorithms have been proposed for the solution of inverse problems associated with the steady-state heat conduction in the absence of heat sources for isotropic materials, see Ingham and Yuan (1994), Lesnic, Elliott and Ingham (1997), and Hào and Lesnic (2000), anisotropic media, see Mera, Elliott, Ingham and Lesnic (2000; 2002), and heat conduction in fins, see Marin, Elliott, Heggs, Ingham, Lesnic and Wen (2003a; 2003b; 2004). Recently, the MFS has been successfully applied to solving inverse problems associated with the heat equation, see Hon and Wei (2004) and

Mera (2005), linear elasticity, see Marin and Lesnic (2004) and Marin (2005a), steady-state heat conduction in functionally graded materials, see Marin (2005b), Helmholtz-type equations, see Marin and Lesnic (2005), Marin (2005c), and Jin and Zheng (2006), and source reconstruction in steady-state heat conduction problems, see Jin and Marin (2007).

To the best of our knowledge, the application of the MFS to inverse boundary value problems associated with the Poisson equation has not been investigated as yet. Motivated by the recent encouraging results of the MFS applications to inverse problems and using the approach proposed by Alves and Chen (2005), the inverse boundary value problems for the Poisson equation are solved in two steps. Firstly, an approximate MFS particular solution of the Poisson equation is sought. The solution of the resulting inverse boundary value problem for the Laplace equation is then found using a classical MFS. The resulting MFS discretised system of equations for the later inverse boundary value problem is ill-conditioned and hence it is solved by employing the SVD, see Hansen (1998), whilst the choice of the regularization parameter is based on the L-curve criterion, see Hansen (2001). Three examples for the Poisson equation in smooth and piecewise smooth, simply and doubly connected, two-dimensional domains are considered, whilst the convergence and stability of the method are carefully investigated based on the numerical examples analysed.

2 Mathematical formulation

Let Ω be an open bounded domain in \mathbb{R}^d , where d is the dimensionality of the space, and $\partial\Omega$ its boundary. In the presence of heat sources, $f(\mathbf{x})$, $\mathbf{x} = (x_1, \dots, x_d) \in \Omega$, the steady-state heat conduction in an isotropic medium is described by the Poisson equation, see e.g. Kraus, Aziz and Welty (2001), and Beck, Blackwell and St. Clair (1985), namely

$$\Delta u(\mathbf{x}) \equiv \sum_{i=1}^d \frac{\partial^2 u(\mathbf{x})}{\partial x_i^2} = f(\mathbf{x}), \quad \mathbf{x} \in \Omega, \quad (1)$$

where $u(\mathbf{x})$ denotes the temperature at $\mathbf{x} \in \Omega$. The normal heat flux through the boundary $\partial\Omega$ is given by

$$\phi(\mathbf{x}) \equiv \nabla u(\mathbf{x}) \cdot \mathbf{n}(\mathbf{x}) = \sum_{i=1}^d \frac{\partial u(\mathbf{x})}{\partial x_i} n_i(\mathbf{x}), \quad \mathbf{x} \in \partial\Omega, \quad (2)$$

where $\mathbf{n}(\mathbf{x}) = (n_1(\mathbf{x}), \dots, n_d(\mathbf{x}))^T$ is the outward unit normal vector at $\mathbf{x} \in \partial\Omega$.

In this paper, we investigate the following inverse problem:

$$\Delta u(\mathbf{x}) = f(\mathbf{x}), \quad \mathbf{x} \in \Omega \quad (3.1)$$

$$u(\mathbf{x}) = \tilde{u}(\mathbf{x}), \quad \mathbf{x} \in \Gamma_D \quad (3.2)$$

$$\phi(\mathbf{x}) = \tilde{\phi}(\mathbf{x}), \quad \mathbf{x} \in \Gamma_N \quad (3.3)$$

$$u(\mathbf{x}) = \tilde{u}(\mathbf{x}), \quad \mathbf{x} \in \Omega_{\text{int}} \quad (3.4)$$

where $\Gamma_D \subset \partial\Omega$, $\Gamma_N \subset \partial\Omega$ and $\Omega_{\text{int}} \subset \Omega$. Furthermore, the following formulations associated with the inverse problem (3.1) – (3.4) can occur, see also Figs. 1(a)–(d):

Formulation 1: $\Gamma_D \neq \emptyset$; $\Gamma_N \neq \emptyset$; $\Gamma_D = \Gamma_N$; $\Omega_{\text{int}} = \emptyset$.

Formulation 2: $\Gamma_D \neq \emptyset$; $\Gamma_N \neq \emptyset$; $\Gamma_N \subset \Gamma_D$; $\Omega_{\text{int}} = \emptyset$.

Formulation 3: $\Gamma_D = \emptyset$; $\Gamma_N \neq \emptyset$; $\Omega_{\text{int}} \neq \emptyset$.

More precisely, Formulations 1 – 3 describe the following inverse problems associated with the steady-state heat conduction in the presence of sources: Formulation 1 represents the classical Cauchy problem for the Poisson equation, in which both the temperature and normal heat flux can be measured on a part of the boundary $\partial\Omega$, see Figs. 1(a) and (d). Formulation 2 provides us with more information than Formulation 1, in the sense that apart from the boundary data which are also available in the Cauchy problem, additional boundary temperature measurements can be made, see Fig. 1(c). Although not presented herein, it should be mentioned that another inverse problem, similar to that described by Formulation 2 and in which the additional boundary temperature measurements available in the aforementioned formulation are replaced by extra

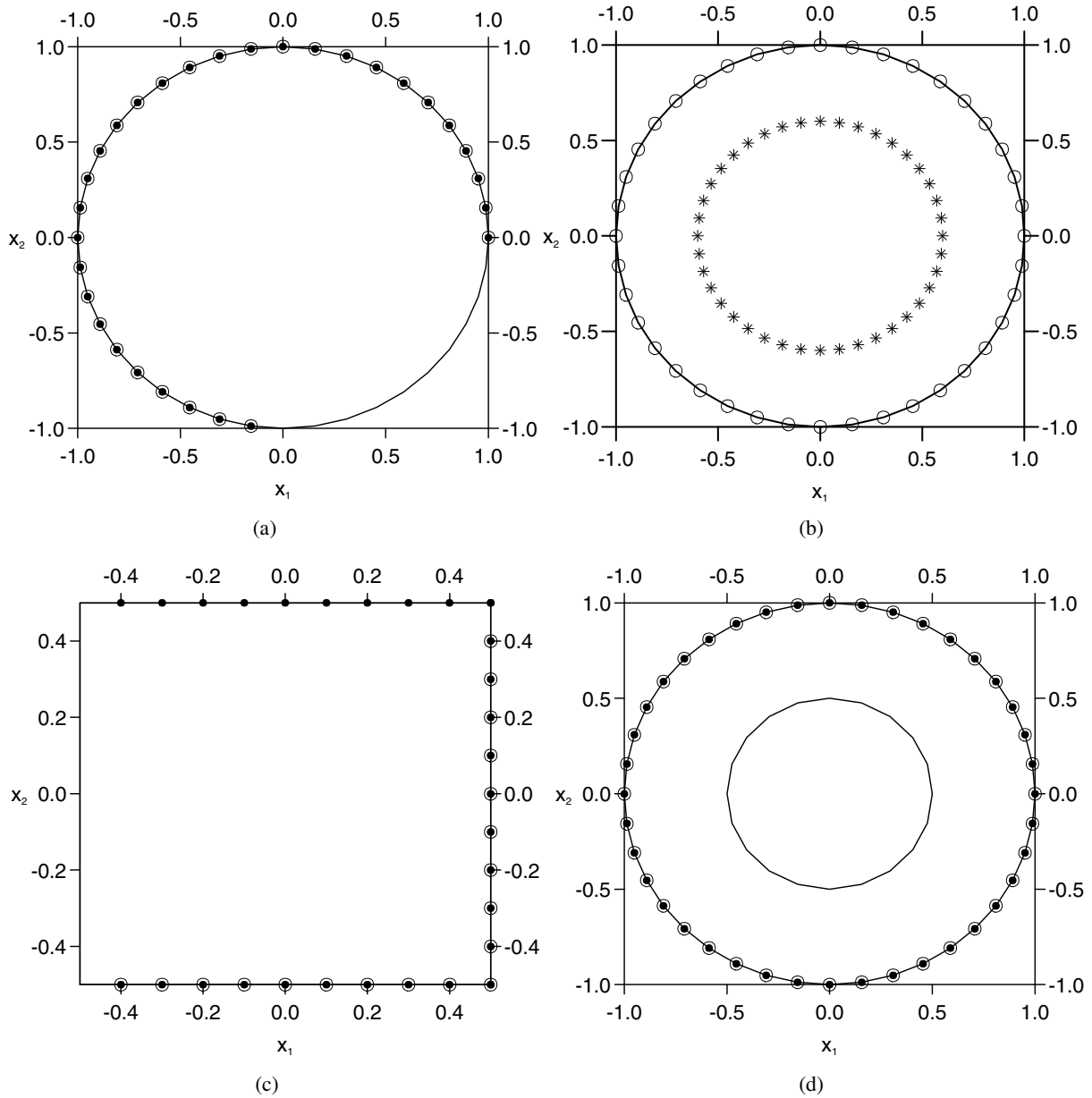


Figure 1: Schematic diagram of the examples and formulations analysed, namely (a) Example 1, Formulation 1, (b) Example 1, Formulation 3, (c) Example 2, Formulation 2, and (d) Example 3, Formulation 1, with given Dirichlet (●), Neumann (○) and internal (*) data, respectively.

boundary flux measurements, can also be considered, namely:

Formulation 2' : $\Gamma_D \neq \emptyset$; $\Gamma_N \neq \emptyset$; $\Gamma_D \subset \Gamma_N$; $\Omega_{int} = \emptyset$.

Finally, Formulation 3 is concerned with the situation when the flux is known on a portion Γ_N of the boundary $\partial\Omega$ such that Γ_N encloses the domain

Ω , whilst temperature measurements are available in $\Omega_{int} \subset \Omega$ such that the internal domain Ω_{int} is bounded by a closed curve, see Fig. 1(b).

The inverse problem (3.1) – (3.4) for Formulations 1 – 3 is much more difficult to solve both analytically and numerically than the direct problem since the solution does not satisfy the general conditions of well-posedness. It is well-known that if

this solution exists then it is unstable with respect to small perturbations in the data on Γ_D and/or Γ_N , see e.g. Hadamard (1923). Thus the problem under investigation is ill-posed and we cannot use a direct approach, such as the Gauss elimination method, in order to solve the system of linear equations which arises from the discretisation of the partial differential equation (3.1), and the boundary and internal conditions (3.2) – (3.4). Therefore, regularization methods are required to solve accurately the inverse problem (3.1) – (3.4) for the associated Formulations 1 – 3.

3 Approximate solution of the inverse problem

Following the approach of Alves and Chen (2005), the extension of the method of fundamental solutions (MFS) for the solution of the Laplace equation to the solution of the Poisson equation, i.e. inhomogeneous Laplace equation, is presented in this section. The main idea consists of finding a particular solution of the inhomogeneous equation (Poisson equation) and then solving a boundary value problem for the associated homogeneous equation (Laplace equation), where the boundary conditions are obtained using the boundary conditions for the original inhomogeneous equation (Poisson equation) and the values of the particular solution previously obtained on the boundary. The particular and homogeneous solutions can then be approximated using the MFS.

3.1 Superposition principle

On using the linearity of the Laplacian operator, Δ , the superposition principle can be applied to the inverse boundary value problem (3.1) – (3.4) and hence its solution can be written as

$$u(\mathbf{x}) = u_p(\mathbf{x}) + u_h(\mathbf{x}), \quad \mathbf{x} \in \Omega, \quad (4)$$

where $u_p(\mathbf{x})$ is a particular solution of the Poisson equation (3.1), whilst $u_h(\mathbf{x})$ is the homogeneous solution to the resulting boundary value problem for the Laplace equation. More precisely, $u_p(\mathbf{x})$ satisfies the Poisson equation

$$\Delta u_p(\mathbf{x}) = f(\mathbf{x}), \quad \mathbf{x} \in \Omega, \quad (5)$$

but does not necessarily satisfy the boundary conditions (3.2) and (3.3), nor the additional internal measurements (3.4) corresponding to the original problem. From Eq. (4) we obtain

$$u_h(\mathbf{x}) = u(\mathbf{x}) - u_p(\mathbf{x}), \quad \mathbf{x} \in \Omega. \quad (6)$$

Hence on using Eqs. (3.1) – (3.4), (5) and (6), it follows that $u_h(\mathbf{x})$ is the solution of the following boundary value problem for the Laplace equation

$$\Delta u_h(\mathbf{x}) = 0, \quad \mathbf{x} \in \Omega \quad (7.1)$$

$$u_h(\mathbf{x}) = \tilde{u}(\mathbf{x}) - u_p(\mathbf{x}), \quad \mathbf{x} \in \Gamma_D \quad (7.2)$$

$$\phi_h(\mathbf{x}) = \tilde{\phi}(\mathbf{x}) - \phi_p(\mathbf{x}), \quad \mathbf{x} \in \Gamma_N \quad (7.3)$$

$$u_h(\mathbf{x}) = \tilde{u}(\mathbf{x}) - u_p(\mathbf{x}), \quad \mathbf{x} \in \Omega_{\text{int}} \quad (7.4)$$

where $\phi_h(\mathbf{x}) \equiv \nabla u_h(\mathbf{x}) \cdot \mathbf{n}(\mathbf{x})$, $\mathbf{x} \in \Gamma_N$, and $\phi_p(\mathbf{x}) \equiv \nabla u_p(\mathbf{x}) \cdot \mathbf{n}(\mathbf{x})$, $\mathbf{x} \in \Gamma_N$.

3.2 Approximate solution of the homogeneous equation

The fundamental solution of the two-dimensional Laplace equation, i.e. Eq. (7.1) with $d = 2$, is given by, see e.g. Berger and Karageorghis (1999),

$$\mathcal{F}(\mathbf{x}, \mathbf{y}) = \frac{1}{2\pi} \ln \frac{1}{r(\mathbf{x}, \mathbf{y})}, \quad \mathbf{x} \in \overline{\Omega}, \quad \mathbf{y} \in \mathbb{R}^2 \setminus \overline{\Omega}, \quad (8)$$

where $r(\mathbf{x}, \mathbf{y}) = \sqrt{(x_1 - y_1)^2 + (x_2 - y_2)^2}$ represents the distance between the domain point $\mathbf{x} = (x_1, x_2)$ and the MFS source point or singularity $\mathbf{y} = (y_1, y_2)$.

The main idea in the MFS consists of approximating the temperature in the solution domain by a linear combination of fundamental solutions with respect to n_s singularities \mathbf{y}^j in the form

$$u_h(\mathbf{x}) \approx \sum_{j=1}^{n_s} c_j \mathcal{F}(\mathbf{x}, \mathbf{y}^j), \quad \mathbf{x} \in \overline{\Omega}, \quad (9)$$

where $\mathbf{c} = (c_1, \dots, c_{n_s})$ and \mathbf{Y} is a $(2n_s)$ -vector containing the Cartesian coordinates of the singularities \mathbf{y}^j , $j = 1, \dots, n_s$. Then the normal heat flux on the boundary $\partial\Omega$ can be approximated by

$$\phi_h(\mathbf{x}) \approx \sum_{j=1}^{n_s} c_j \mathcal{G}(\mathbf{x}, \mathbf{y}^j), \quad \mathbf{x} \in \partial\Omega, \quad (10)$$

where $\mathcal{G}(\mathbf{x}, \mathbf{y}) = \nabla_{\mathbf{x}} \mathcal{F}(\mathbf{x}, \mathbf{y}) \cdot \mathbf{n}(\mathbf{x})$ is given by

$$\mathcal{G}(\mathbf{x}, \mathbf{y}) = -\frac{(\mathbf{x} - \mathbf{y})^T \cdot \mathbf{n}(\mathbf{x})}{2\pi r^2(\mathbf{x}, \mathbf{y})}, \quad \mathbf{x} \in \partial\Omega, \quad \mathbf{y} \in \mathbb{R}^2 \setminus \overline{\Omega}. \quad (11)$$

If n_D collocation points \mathbf{x}^i , $i = 1, \dots, n_D$, and n_N collocation points \mathbf{x}^{n_D+i} , $i = 1, \dots, n_N$, are chosen on the boundaries Γ_D and Γ_N , respectively, the temperature measurements are available at n_{int} internal points $\mathbf{x}^{n_D+n_N+i}$, $i = 1, \dots, n_{\text{int}}$, in Ω_{int} , and the location of the singularities \mathbf{y}^j , $j = 1, \dots, n_s$, is set then Eqs. (3.2) – (3.4) recast as a system of $(n_D + n_N + n_{\text{int}})$ linear algebraic equations with n_s unknowns which can be generically written as

$$\mathbf{A}\mathbf{c} = \mathbf{F}, \quad (12)$$

where the components of the MFS matrix $\mathbf{A} \in \mathbb{R}^{(n_D+n_N+n_{\text{int}}) \times n_s}$ and the right-hand side vector $\mathbf{F} \in \mathbb{R}^{n_D+n_N+n_{\text{int}}}$ are given by

$$A_{ij} = \begin{cases} \mathcal{F}(\mathbf{x}^i, \mathbf{y}^j), & 1 \leq i \leq n_D, \\ & 1 \leq j \leq n_s \\ \mathcal{G}(\mathbf{x}^i, \mathbf{y}^j), & 1 \leq i - n_D \leq n_N, \\ & 1 \leq j \leq n_s \\ \mathcal{F}(\mathbf{x}^i, \mathbf{y}^j), & 1 \leq i - n_D - n_N \leq n_{\text{int}}, \\ & 1 \leq j \leq n_s \end{cases} \quad (13)$$

and

$$F_i = \begin{cases} \tilde{u}(\mathbf{x}^i) - u_p(\mathbf{x}^i), & 1 \leq i \leq n_D \\ \tilde{\phi}(\mathbf{x}^i) - \phi_p(\mathbf{x}^i), & 1 \leq i - n_D \leq n_N \\ \tilde{u}(\mathbf{x}^i) - u_p(\mathbf{x}^i), & 1 \leq i - n_D - n_N \leq n_{\text{int}} \end{cases} \quad (14)$$

respectively.

It should be noted that in order to uniquely determine the solution \mathbf{c} of the system of linear algebraic equations (12), i.e. the coefficients c_j , $j = 1, \dots, n_s$, in approximations (9) and (10), the numbers of collocation points corresponding to the Dirichlet and Neuman boundary conditions, and internal temperature measurements, n_D , n_N and n_{int} , respectively, and the number of singularities, n_s , must satisfy the inequality $n_s \leq n_D + n_N + n_{\text{int}}$. However, the system of linear algebraic equations (12) cannot be solved by direct

methods, such as the least-squares method, since such an approach would produce a highly unstable solution due to the large value of the condition number of the matrix \mathbf{A} , which increases dramatically as the number of boundary and internal collocation points, and singularities increases. Several regularization procedures have been developed to solve this type of ill-conditioned systems, such as the Tikhonov regularization method, see Tikhonov and Arsenin (1986), the singular value decomposition (SVD), see Hansen (1998), etc. For a comprehensive study devoted to the application of the MFS, in conjunction with several regularization techniques, for solving numerically the Cauchy problem associated with elliptic operators, we refer the reader to the recent paper of Wei, Hon and Ling (2007). However, in the present study, we only consider the SVD and this is discussed in detail in Section 4.1.

3.3 Approximate particular solution

In the case of the solution of inhomogeneous equations, the MFS must be coupled with other methods that can provide an approximate particular solution. In the BEM literature, the most successful methods are the dual reciprocity method (DRM), see e.g. Nardini and Brebbia (1982) and Partridge, Brebbia and Wrobel (1992), and the multiple reciprocity method (MRM), see e.g. Nowak and Neves (1994). In particular, radial basis functions (RBF) and thin plate splines (TPS) have been widely used in the DRM approach, see e.g. Golberg and Chen (1994; 1999). For other methods used in the approximation of particular solutions, we refer the reader to the comprehensive reviews of Golberg (1995) and Golberg and Chen (1999).

Recently, Alves and Chen (2005) proposed the use of the eigenfunctions associated with the differential operator to approximate a particular solution and presented an extended MFS for solving inhomogeneous problems in a unified manner. This method seems to be very promising considering the numerical results presented therein. Motivated by these results, we attempt to solve the inverse problem (3.1) – (3.4) by the extended MFS. The main idea of Alves and Chen (2005) consists

of approximating the term $f(\mathbf{x})$ by a linear combination of the eigenvalues associated with the Laplacian operator, Δ , namely

$$f(\mathbf{x}) \approx \sum_{k=1}^{n_f} \sum_{j=1}^{n_{ds}} a_{jk} \Psi_{\lambda_k}(\mathbf{x}, \tilde{\mathbf{y}}^j), \quad \mathbf{x} \in \Omega. \quad (15)$$

Here n_f is the number of frequencies, n_{ds} is the number of source points, a_{jk} , $j = 1, \dots, n_{ds}$, $k = 1, \dots, n_f$, are coefficients to be determined, λ_k , $k = 1, \dots, n_f$, are the eigenvalues of the Laplacian operator, Ψ_{λ_k} , $k = 1, \dots, n_f$, are the eigenfunctions of the Laplacian operator corresponding to the aforementioned eigenvalues and $\tilde{\mathbf{y}}^j$, $j = 1, \dots, n_{ds}$, are the source points.

Since Ψ_{λ_k} is the eigenfunction of the Laplacian operator corresponding to the eigenvalue λ_k , for every $k = 1, \dots, n_f$, it satisfies the following eigenequation:

$$\Delta_{\mathbf{x}} \Psi_{\lambda_k}(\mathbf{x}, \tilde{\mathbf{y}}^j) = \lambda_k \Psi_{\lambda_k}(\mathbf{x}, \tilde{\mathbf{y}}^j), \quad \mathbf{x} \in \Omega. \quad (16)$$

Moreover, we take the eigenfunctions Ψ_{λ_k} , $k = 1, \dots, n_f$, to be the fundamental solution of the two-dimensional Helmholtz equation (16) with $\lambda_k < 0$, $k = 1, \dots, n_f$, namely

$$\Psi_{\lambda_k}(\mathbf{x}, \tilde{\mathbf{y}}^j) = \frac{i}{4} H_0^{(1)} \left(\sqrt{-\lambda_k} r(\mathbf{x}, \tilde{\mathbf{y}}^j) \right), \quad \mathbf{x} \in \bar{\Omega}, \quad \tilde{\mathbf{y}}^j \in \mathbb{R}^2 \setminus \bar{\Omega}, \quad (17)$$

where $H_0^{(1)}$ is the Hankel function of the first kind of order zero. Recall that $H_0^{(1)} = J_0 + iY_0$, where J_0 and Y_0 are the Bessel functions of the first and second kind, respectively. Furthermore, J_0 is analytic everywhere, while Y_0 exhibits a logarithmic singular behaviour at zero. Therefore, another alternative is to use the Bessel function J_0 instead of $H_0^{(1)}$ in equation (17) and consider the source points $\tilde{\mathbf{y}}^j$, $j = 1, \dots, n_{ds}$, also inside the domain Ω , i.e.

$$\Psi_{\lambda_k}(\mathbf{x}, \tilde{\mathbf{y}}^j) = J_0 \left(\sqrt{-\lambda_k} r(\mathbf{x}, \tilde{\mathbf{y}}^j) \right), \quad \mathbf{x} \in \bar{\Omega}, \quad \tilde{\mathbf{y}}^j \in \Omega. \quad (18)$$

Thus we obtain the following approximation for the particular solution $u_p(\mathbf{x})$ of Eq. (5):

$$u_p(\mathbf{x}) \approx \sum_{k=1}^{n_f} \sum_{j=1}^{n_{ds}} \frac{a_{jk}}{-\lambda_k} \Psi_{\lambda_k}(\mathbf{x}, \tilde{\mathbf{y}}^j), \quad \mathbf{x} \in \Omega. \quad (19)$$

The use of the fundamental solutions of the eigenequations (16) to approximate a particular solution to the Poisson equation (5) has been justified by Alves and Chen (2005). Since the function $f(\mathbf{x})$, $\mathbf{x} \in \Omega$, is known, the unknown coefficients a_{jk} , $j = 1, \dots, n_{ds}$, $k = 1, \dots, n_f$, are determined by collocating Eq. (15) according to the following algorithm, see Alves and Chen (2005):

- (i) Choose n_{dc} collocation points, $\tilde{\mathbf{x}}^i$, $i = 1, \dots, n_{dc}$, in the domain Ω . Usually, one chooses $\tilde{\mathbf{x}}^i \in \tilde{\Omega}$, $i = 1, \dots, n_{dc}$, where $\Omega \subset \tilde{\Omega}$.
- (ii) Choose n_{ds} source points, $\tilde{\mathbf{y}}^j$, $j = 1, \dots, n_{ds}$, in $\mathbb{R}^2 \setminus \bar{\Omega}$ if Eq. (17) is used. If Eq. (18) is employed then one may even choose $\tilde{\mathbf{y}}^j \in \Omega$, $j = 1, \dots, n_{ds}$.
- (iii) Choose n_f frequencies, $\lambda_k < 0$, $k = 1, \dots, n_f$.
- (iv) Define the matrix

$$\mathbf{M} = \begin{bmatrix} [\Psi_{\lambda_1}(\tilde{\mathbf{x}}^1, \tilde{\mathbf{y}}^1)] & \dots & [\Psi_{\lambda_{n_f}}(\tilde{\mathbf{x}}^1, \tilde{\mathbf{y}}^1)] \\ \vdots & & \vdots \\ [\Psi_{\lambda_1}(\tilde{\mathbf{x}}^{n_{dc}}, \tilde{\mathbf{y}}^1)] & \dots & [\Psi_{\lambda_{n_f}}(\tilde{\mathbf{x}}^{n_{dc}}, \tilde{\mathbf{y}}^1)] \end{bmatrix} \in \mathbb{R}^{n_{dc} \times (n_f n_{ds})}, \quad (20)$$

where $[\Psi_{\lambda_k}(\tilde{\mathbf{x}}^i, \tilde{\mathbf{y}}^j)] \in \mathbb{R}^{n_{dc} \times n_{ds}}$, $k = 1, \dots, n_f$.

- (v) Solve the $(n_f n_{ds}) \times (n_f n_{ds})$ least-squares system

$$\mathbf{M}^T \mathbf{M} \mathbf{a} = \mathbf{M}^T \mathbf{f}, \quad (21)$$

to determine the unknown coefficients $\mathbf{a} = (a_{jk})^T \in \mathbb{R}^{n_f n_{ds}}$, where $\mathbf{f} = (f(\tilde{\mathbf{x}}^1), \dots, f(\tilde{\mathbf{x}}^{n_{dc}}))^T \in \mathbb{R}^{n_{dc}}$.

- (vi) Determine the approximation of the particular solution $u_p(\mathbf{x})$ from Eq. (19).

It should be mentioned that for each frequency, $\lambda_k < 0$, $k = 1, \dots, n_f$, one might consider different source points, $\tilde{\mathbf{y}}^j$, $j = 1, \dots, n_{ds}$. The theoretical density result proved by Alves and Chen (2005) does not specify a precise location of the source points, $\tilde{\mathbf{y}}^j$, $j = 1, \dots, n_{ds}$, in $\mathbb{R}^2 \setminus \bar{\Omega}$ or Ω . Therefore, we might also consider the location of the source points as an unknown to the minimisation problem. However, this implies to consider a nonlinear minimisation problem, instead of considering a simple least-squares method, see Fairweather and Karageorghis (1998). To keep the

simplicity of the method, we will only consider the same fixed source points, $\tilde{\mathbf{y}}^j$, $j = 1, \dots, n_{ds}$, in $\mathbb{R}^2 \setminus \bar{\Omega}$ or Ω for all the frequencies chosen, $\lambda_k < 0$, $k = 1, \dots, n_f$.

4 Regularization

In order to implement the MFS, the location of the source points/singularities has to be determined and this is usually achieved by considering either the static or the dynamic approach. In the static approach, the source points/singularities are pre-assigned and kept fixed throughout the solution process, whilst in the dynamic approach, the source points/singularities and the unknown coefficients are determined simultaneously during the solution process, see Fairweather and Karageorghis (1998). For nonlinear systems, the uniqueness of the solution is not always guaranteed and it is computationally much more expensive. In addition, the discretised MFS system is severely ill-posed in the case of inverse problems and thus the dynamic approach transforms the problem into a more difficult nonlinear ill-posed problem. The dynamic approach results in a system of nonlinear equations, which may be solved using minimization methods. Alternatively, Tankelevich, Fairweather, Karageorghis and Smyrlis (2006), consider the source points located on a so-called pseudo-boundary, which has the same shape as the boundary of the domain, and the problem is solved for a sequence of such pseudo-boundaries, whilst the optimal pseudo-boundary is taken to be the one for which boundary conditions are satisfied most accurately. From a computational point of view, the dynamic approach might not be appropriate for inverse problems with noisy data. Moreover, Mitic and Rashed (2004) have shown that the distribution and number of the source points/singularities are not, in general, important under certain conditions, in the sense that the number of sources/singularities should reflect the degrees of freedom inherent in the boundary conditions of the problem. Hence the dynamic approach for determining the optimal location of the source points/singularities might be unnecessary. Therefore, we have decided to employ the static

approach in our computations.

The MFS can be regarded as a Fredholm integral equation of the first kind with an analytical kernel function, see e.g. Golberg and Chen (1999), which is severely ill-posed according to the theory of integral equations, see e.g. Kress (1989). Consequently, as an approximation to the integral operator, the discretisation matrix \mathbf{A} is severely ill-conditioned. The accurate and stable solution of Eq. (12) is very important for obtaining physically meaningful numerical results. Regularization methods are among the most popular and successful methods for solving stably and accurately ill-conditioned matrix equations, see Hansen (1998) and Tikhonov and Arsenin (1986). In our computations we use the truncated SVD to solve the matrix equation arising from the MFS discretisation.

4.1 Singular value decomposition

The SVD of a matrix $\mathbf{A} \in \mathbb{R}^{(n_D+n_N+n_{int}) \times n_s}$, $n_s \leq n_D + n_N + n_{int}$, is given by, see e.g. Hansen (1998),

$$\mathbf{A} = \mathbf{U}\mathbf{\Sigma}\mathbf{V}^T, \quad (22)$$

where $\mathbf{U} = [\mathbf{u}_1, \mathbf{u}_2, \dots, \mathbf{u}_{n_D+n_N+n_{int}}]$ and $\mathbf{V} = [\mathbf{v}_1, \mathbf{v}_2, \dots, \mathbf{v}_{n_s}]$ are orthonormal matrices with column vectors called the left and the right singular vectors, respectively, T denotes the matrix transposition and $\mathbf{\Sigma} = \text{diag}(\sigma_1, \sigma_2, \dots, \sigma_{n_s})$ is a diagonal matrix with nonnegative diagonal elements in non-increasing order, which are the singular values of \mathbf{A} .

On using the SVD, the solution \mathbf{c} to the matrix equation (12) can be succinctly written as a linear combination of the right singular vectors, namely

$$\mathbf{c} = \sum_{i=1}^{\text{rank}(\mathbf{A})} \frac{\mathbf{u}_i^T \mathbf{F}}{\sigma_i} \mathbf{v}_i, \quad (23)$$

where $\text{rank}(\mathbf{A})$ is the rank of the matrix \mathbf{A} . For an ill-conditioned matrix equation, there are many small singular values clustering around zero and therefore the solution obtained by standard methods, such as the Gauss elimination method, may be dominated by the contribution of the small singular values and hence it becomes unbounded and oscillatory. One simple remedy is to truncate the

above summation, i.e. by considering an approximate solution, \mathbf{c}_n , given by

$$\mathbf{c}_n = \sum_{i=1}^n \frac{\mathbf{u}_i^T \mathbf{F}}{\sigma_i} \mathbf{v}_i, \quad (24)$$

where $n \leq \text{rank}(\mathbf{A})$ is the regularization parameter which determines when one starts to leave out small singular values. This method is known as the truncated SVD (TSVD) in the inverse problem community, see Hansen (1998).

The performance of regularization methods depends crucially on the suitable choice of the regularization parameter. One extensively studied criterion is the discrepancy principle, see e.g. Morozov (1996). Although this criterion is mathematically rigorous, it requires a reliable estimation of the amount of noise added into the data which may not be available in practical problems. Heuristical approaches are preferable in the case when no *a priori* information about the noise is available. For the TSVD, several heuristical approaches have been proposed, including the L-curve criterion, see Hansen (1998; 2001), and the generalized cross-validation, see Wahba (1977). In this paper, we employ the L-curve criterion to determine the appropriate regularization parameter for the TSVD, see Hansen (1998; 2001).

If we define the curve

$$\{(\|\mathbf{c}_n\|_2, \|\mathbf{A}\mathbf{c}_n - \mathbf{F}\|_2) \mid n = 1, 2, \dots, \text{rank}(\mathbf{A})\} \quad (25)$$

on a logarithmic scale then this typically has an L-shaped form and hence it is known as the L-curve. According to the L-curve criterion, the optimal regularization parameter corresponds to the corner of the L-curve since a good tradeoff between the residual and solution norms is achieved at this point. Numerically, the L-curve method is robust and stable with respect to both uncorrelated and highly correlated noise. Furthermore, this criterion works effectively with certain classes of practical problems, see Hansen (1998; 2001) and Chen, Chen, Hong and Chen (1995). For a discussion of the theoretical aspects of the L-curve criterion, we refer the reader to Hanke (1996) and Vogel (1996).

Several algorithms for locating the corner of the L-curve have been reported in the literature, see e.g. Hansen (2001), Guerra and Hernandez (2001), Kaufman and Neumaier (1996) and Castellanos, Gomez and Guerra (2002). The first procedure is based on fitting a parametric cubic spline to the discrete points and then taking the point corresponding to the maximum curvature of the L-curve to be its corner, see Hansen (2001). The second algorithm employs a conic to fit the set of discrete points, see Guerra and Hernandez (2001), whilst the third one is based on using a linear-linear scale and inverting the axis, see Kaufman and Neumaier (1996). All these procedures need to check the monotonicity condition for the sequences of the residual and solution norms, and discard those points where the monotonicity condition is not fulfilled. The last algorithm, namely the triangle method, is based on geometric considerations, see e.g. Castellanos, Gomez and Guerra (2002). In the present study, we mainly employ the first algorithm. However, the curvature of the parametric spline is very sensitive to the distribution of the collocation points and occasionally the located corner is not suitable, see Hansen (2001). Therefore, visual inspection is used as an auxiliary procedure.

5 Numerical results and discussion

In this section, we present the numerical results obtained using the MFS described in Section 3, in conjunction with the SVD presented in Section 4.1, for Formulations 1 – 3 of the inverse problem (3.1) – (3.4) associated with the steady-state isotropic heat conduction in smooth and piecewise smooth, simply and doubly connected, two-dimensional domains. We investigate the convergence of the proposed numerical method with respect to the number of singularities and the distance from the singularities to the boundary of the solution domain. We also analyse the stability of the MFS+SVD algorithm as a function of the level of noise added into the boundary and/or internal data. In addition, we perform a sensitivity analysis with respect to the number of frequencies used to approximate the particular temperature solution $u_p(\mathbf{x})$.

5.1 Examples

In order to present the performance of the combined MFS+SVD algorithm for solving the inverse problem given by Eqs. (3.1) – (3.4), we consider the following examples, see also Figs. 1(a)–(d):

Example 1 (Smooth, simply connected domain): We consider the disk $\Omega = \{\mathbf{x} \in \mathbb{R}^2 \mid x_1^2 + x_2^2 < r^2\}$, where $r = 1.0$, and the following analytical solutions for the temperature and the normal heat flux

$$u^{(\text{an})}(\mathbf{x}) = x_1 x_2 \sin(x_1 x_2) \quad (26)$$

and

$$\begin{aligned} \phi^{(\text{an})}(\mathbf{x}) = & [\sin(x_1 x_2) + x_1 x_2 \cos(x_1 x_2)] x_2 \mathbf{n}_1(\mathbf{x}) \\ & + [\sin(x_1 x_2) + x_1 x_2 \cos(x_1 x_2)] x_1 \mathbf{n}_2(\mathbf{x}), \end{aligned} \quad (27)$$

respectively. Here the right-hand side of Eq. (3.1) is given by

$$f(\mathbf{x}) = (x_1^2 + x_2^2)[2 \cos(x_1 x_2) - x_1 x_2 \sin(x_1 x_2)] \quad (28)$$

and we investigate the following formulations

Formulation 1:

$$\begin{aligned} \Gamma_D = & \{\mathbf{x} \in \partial\Omega \mid 0 \leq \theta(\mathbf{x}) < 3\pi/2, \rho(\mathbf{x}) = r\}, \\ \Gamma_N = & \Gamma_D, \quad \Omega_{\text{int}} = \emptyset, \end{aligned} \quad (29)$$

Formulation 3:

$$\begin{aligned} \Gamma_D = & \emptyset, \\ \Gamma_N = & \partial\Omega \\ = & \{\mathbf{x} \in \partial\Omega \mid 0 \leq \theta(\mathbf{x}) < 2\pi, \rho(\mathbf{x}) = r\}, \\ \Omega_{\text{int}} = & \\ \left\{ \mathbf{x}^j \in \Omega \mid \right. & \left. \begin{aligned} \theta(\mathbf{x}^j) = & 2j\pi/n_{\text{int}}, \\ \rho(\mathbf{x}^j) = & \rho_j, \quad j = 0, 1, \dots, n_{\text{int}} - 1 \end{aligned} \right\}, \\ \rho_j = & 0.5, \quad j = 0, 1, \dots, n_{\text{int}} - 1. \end{aligned} \quad (30)$$

Here $\rho(\mathbf{x})$ and $\theta(\mathbf{x})$ are the polar coordinates of $\mathbf{x} \in \mathbb{R}^2$.

Example 2 (Piecewise smooth, simply connected domain): We consider the square $\Omega = (-0.5, 0.5)^2$ and the following analytical solutions for the temperature and the normal heat flux

$$u^{(\text{an})}(\mathbf{x}) = \sin(x_1) \sinh(x_2) + \cosh(3x_1) + x_1^3 - x_2^2 \quad (31)$$

and

$$\begin{aligned} \phi^{(\text{an})}(\mathbf{x}) = & [\cos(x_1) \sinh(x_2) + 3x_1^2] \mathbf{n}_1(\mathbf{x}) \\ & + [\sin(x_1) \cosh(3x_2) + 3 \sinh(3x_1) - 2x_2] \mathbf{n}_2(\mathbf{x}), \end{aligned} \quad (32)$$

respectively. Here the right-hand side of Eq. (3.1) is given by

$$f(\mathbf{x}) = 9 \cosh(3x_1) + 6x_1 - 2 \quad (33)$$

and we investigate

Formulation 2:

$$\begin{aligned} \Gamma_N = & (-0.5, 0.5] \times \{-0.5\} \cup \{0.5\} \times (-0.5, 0.5), \\ \Gamma_D = & (-0.5, 0.5] \times \{-0.5\} \cup \{0.5\} \times (-0.5, 0.5] \\ & \cup (-0.5, 0.5) \times \{0.5\}, \quad \Omega_{\text{int}} = \emptyset. \end{aligned} \quad (34)$$

Example 3 (Smooth, doubly connected domain): We consider the annulus $\Omega = \{\mathbf{x} \in \mathbb{R}^2 \mid r_i^2 < x_1^2 + x_2^2 < r_o^2\}$, where $r_o = 1.0$ and $r_i = 0.5$, and the following analytical solutions for the temperature and the normal heat flux

$$u^{(\text{an})}(\mathbf{x}) = \exp(-x_1^2 + 2x_2) \quad (35)$$

and

$$\phi^{(\text{an})}(\mathbf{x}) = 2[-x_1 \mathbf{n}_1(\mathbf{x}) + \mathbf{n}_2(\mathbf{x})] \exp(-x_1^2 + 2x_2), \quad (36)$$

respectively. The right-hand side of Eq. (3.1) is given by

$$f(\mathbf{x}) = 2(2x_1^2 + 1) \exp(-x_1^2 + 2x_2) \quad (37)$$

and we investigate

Formulation 1:

$$\begin{aligned} \Gamma_D = \Gamma_N = \{ \mathbf{x} \in \partial\Omega \mid x_1^2 + x_2^2 = r_o^2 \}, \\ \Omega_{\text{int}} = \emptyset. \end{aligned} \quad (38)$$

The homogeneous problem (7.1) – (7.4) associated with the various formulations of the inverse problem investigated in this study has been solved using a uniform distribution of the boundary collocation points, \mathbf{x}^i , $i = 1, \dots, n_D$, and \mathbf{x}^{n_D+i} , $i = 1, \dots, n_N$, internal collocation points, $\mathbf{x}^{n_D+n_N+i}$, $i = 1, \dots, n_{\text{int}}$, and the singularities, \mathbf{y}^j , $j = 1, \dots, n_s$, with the latter being located on the boundary of the disk $B(0, r_s)$, where the radius $r_s > 0$ was chosen such that $\tilde{\Omega} \subset B(0, r_s)$. The particular solution (5) corresponding to the inverse problem analysed in this paper has been approximated using Eqs. (18) and (19), and a uniform distribution of both the domain collocation points, $\tilde{\mathbf{x}}^i$, $i = 1, \dots, n_{\text{dc}}$, in the domain $\tilde{\Omega} = (-1.2, 1.2)^2$, such that $\Omega \subset \tilde{\Omega}$, for all examples considered, and the source points, $\tilde{\mathbf{y}}^j$, $j = 1, \dots, n_{\text{ds}}$, in $\hat{\Omega} = (-1.1, 1.1)^2$, such that $\Omega \subset \hat{\Omega}$, whilst the frequencies were taken as $\lambda_k = -k^2$, $k = 1, \dots, n_f$. Unless specified, in the present computations we have set $n_{\text{dc}} = 400$, $n_{\text{ds}} = 16$ and $n_f = 8$ for determining numerically the particular solution u_p .

5.2 Effect of regularization

Before presenting the numerical results obtained using the proposed algorithm, it is interesting to emphasize the necessity of employing regularization methods, instead of standard direct inversion methods, such as the Gauss elimination method, the LU factorization and the least-squares method, in order to obtain stable numerical solutions for the inverse problems under investigation. Chen, Cho and Golberg (2006) have shown that the errors in the numerical solutions to various direct problems for the two-dimensional Laplace equation, obtained using the Gauss elimination method for solving the MFS system of linear algebraic equations, are of the same order as those retrieved by employing the SVD and TSVD, provided that the boundary data are exact.

However, even for a low level of noise added into the boundary data, in the case of various direct problems for the Laplace equation, the TSVD-based solution is superior to that obtained employing the Gauss elimination method and, consequently, this regularization method is recommended to be used, see Chen, Cho and Golberg (2006). Moreover, if an inverse problem for the two-dimensional Laplace equation has to be solved and, in addition, the measured boundary and/or internal data are contaminated by noise then it becomes essential to employ regularization methods, see e.g. Jin (2005). Similar results have been obtained for the MFS applied to solving inverse problems associated with the Lamé system of linear elasticity, Helmholtz-type equations, heat transfer in FGMs, heat conduction etc., see Hon and Wei (2004), Marin and Lesnic (2004; 2005) Mera (2005), Jin and Marin (2005), and Marin (2005a; b; c).

For practical problems the known boundary and/or internal data are inevitably contaminated by measurement errors and thus the stability of the numerical scheme is of vital importance. Therefore, for the examples analysed in this paper the Dirichlet and/or Neumann boundary data $\tilde{u}|_{\Gamma_D}$ and $\tilde{\phi}|_{\Gamma_N}$, respectively, and the internal Dirichlet data, $\tilde{u}|_{\Omega_{\text{int}}}$, have been perturbed as

$$\begin{aligned} \tilde{u}^\delta|_{\Gamma_D} &= \tilde{u}|_{\Gamma_D} + \delta u, & \tilde{\phi}^\delta|_{\Gamma_N} &= \tilde{\phi}|_{\Gamma_N} + \delta \phi, \\ \tilde{u}^\delta|_{\Omega_{\text{int}}} &= \tilde{u}|_{\Omega_{\text{int}}} + \delta u_{\text{int}}, \end{aligned} \quad (39)$$

where δu , $\delta \phi$ and δu_{int} are Gaussian random variables with mean zero and standard deviation $\sigma_u = \max_{\Gamma_D} |u| \times (p_u/100)$, $\sigma_\phi = \max_{\Gamma_N} |\phi| \times (p_\phi/100)$ and $\sigma_{u_{\text{int}}} = \max_{\Omega_{\text{int}}} |u| \times (p_u/100)$, respectively, generated by the NAG subroutine G05DDF, and $p_u, p_\phi \in \{1\%, 2\%, 3\%\}$ are the percentages of additive noise included into the input data $\tilde{u}|_{\Gamma_D}$, $\tilde{\phi}|_{\Gamma_N}$ and $\tilde{u}|_{\Omega_{\text{int}}}$ in order to simulate the inherent measurement errors.

Figs. 2(a) and (b) illustrate the analytical and numerical values for the temperature, u , on the boundary $\partial\Omega \setminus \Gamma_D$ and normal heat flux, ϕ , on the boundary $\partial\Omega \setminus \Gamma_N$, respectively, obtained by the direct inversion of the system of linear algebraic equations.

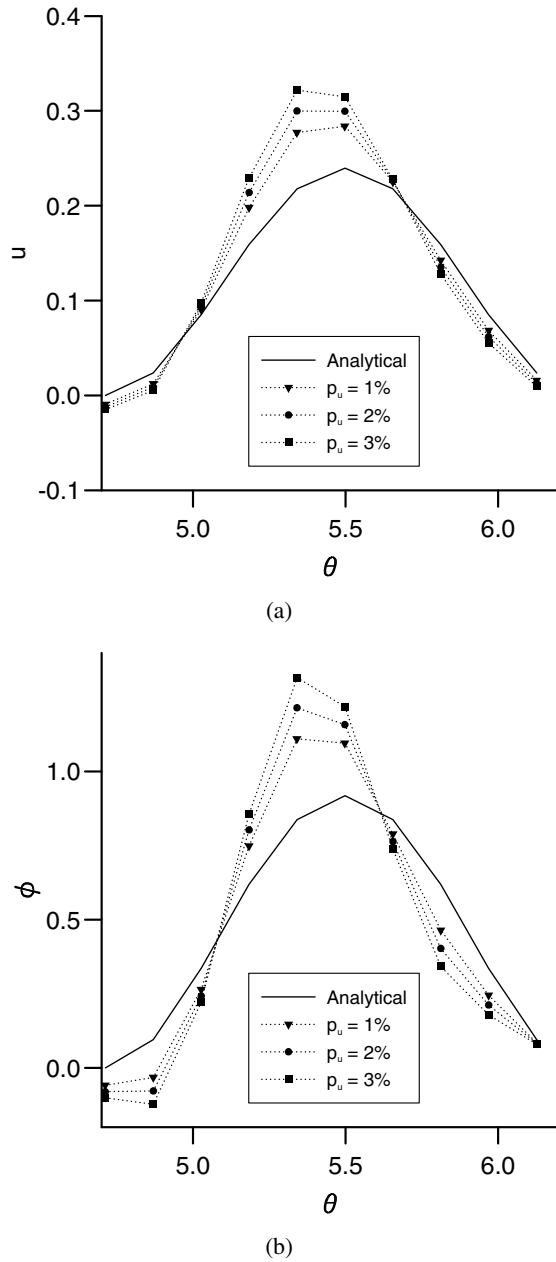


Figure 2: The analytical (—) and the numerical values for (a) the temperature u on the boundary $\partial\Omega \setminus \Gamma_D$, and (b) the normal heat flux ϕ on the boundary $\partial\Omega \setminus \Gamma_N$, obtained with the direct inversion of the system of linear algebraic equation (12) (i.e. the least-squares solution), using $n_D = n_N = 30$ boundary collocation points, $n_{int} = 0$ internal collocation points and $n_s = 60$ singularities for the homogeneous solution u_h , and various levels of noise added into the Dirichlet boundary data $\tilde{u}|_{\Gamma_D}$, namely $p_u = 1\%$ ($\dots \blacktriangledown \dots$), $p_u = 2\%$ ($\dots \bullet \dots$) and $p_u = 3\%$ ($\dots \blacksquare \dots$), in the case of Formulation 1 for Example 1.

braic equation (12) (i.e. the least-squares solution), using $n_D = n_N = 30$ boundary collocation points, $n_{int} = 0$ internal collocation points and $n_s = 60$ singularities for the homogeneous solution u_h , and various levels of noisy Dirichlet data $\tilde{u}|_{\Gamma_D}$, namely $p_u \in \{1\%, 2\%, 3\%\}$, in the case of Formulation 1 for Example 1. From these figures it can be seen that the numerical temperature u on the boundary $\partial\Omega \setminus \Gamma_D$ and the numerical normal heat flux ϕ on the boundary $\partial\Omega \setminus \Gamma_N$ are unstable and hence they represent very inaccurate approximations to their corresponding exact solutions. It should be mentioned that similar results have been obtained for the other inverse problems investigated in this paper and, therefore, they are not presented here. Thus we can conclude that standard direct inversion methods could not yield accurate results for noisy data and, consequently, regularization should be employed to retrieve stable numerical solutions when the input data are contaminated by noise.

5.3 Choice of the optimal regularization parameter

Fig. 3 presents the L-curves obtained with the proposed SVD+MFS method, using $n_D = n_N = 30$ boundary collocation points, $n_{int} = 0$ internal collocation points and $n_s = 60$ singularities for approximating the solution of the homogeneous problem (7.1) – (7.4), and various levels of noise added into the Dirichlet boundary data $\tilde{u}|_{\Gamma_D}$, namely $p_u \in \{1\%, 2\%, 3\%\}$, in the case of Formulation 1 for Example 1. From this figure it can be seen that the corner of the corresponding L-curve can be clearly determined and this gives the truncation numbers $n_{SVD} = 18$ for $p_u = 1\%$ and $n_{SVD} = 19$ for $p_u = 2\%, 3\%$, which represent the optimal values for the regularization parameter. Similar results have been obtained for the other problems investigated in this study and, therefore, they are not presented here.

In order to measure the accuracy of the numerical results obtained with the proposed MFS+SVD algorithm, we use the *root mean square error* for the boundary temperature, $Err_{\Gamma}(u)$, which is de-

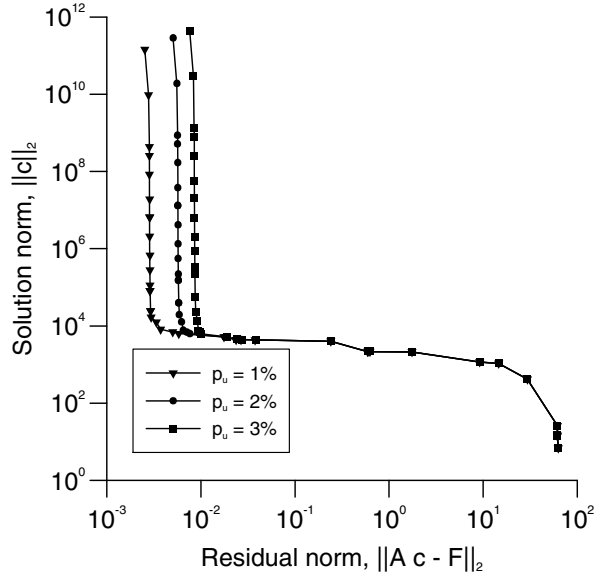


Figure 3: The L-curves obtained using $n_D = n_N = 30$ boundary collocation points, $n_{\text{int}} = 0$ internal collocation points and $n_s = 60$ singularities for the homogeneous solution u_h , and various levels of noise added into the Dirichlet boundary data $\tilde{u}|_{\Gamma_D}$, namely $p_u \in \{1\%, 2\%, 3\%\}$, in the case of Formulation 1 for Example 1.

fined as

$$\text{Err}_{\Gamma}(u) = \frac{\|u^{(\text{an})} - u^{(\text{num})}\|_{L_2(\Gamma)}}{\|u^{(\text{an})}\|_{L_2(\Gamma)}}, \quad (40)$$

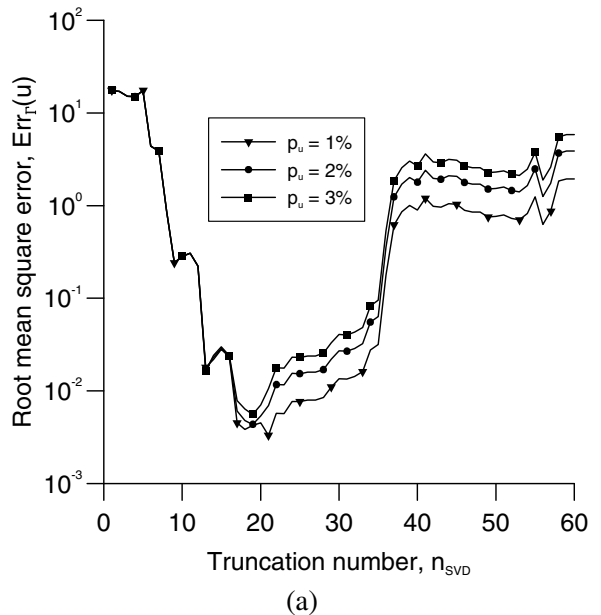
where $u^{(\text{an})}$ and $u^{(\text{num})}$ are the analytical and numerical values for the temperature, respectively, whilst $\|g\|_{L_2(\Gamma)}$ is the discretised L_2 -norm of a function $g(\cdot) : \Gamma \rightarrow \mathbb{R}$ on the boundary $\Gamma \subset \partial\Omega$ and is given by

$$\|g\|_{L_2(\Gamma)}^2 = \sum_{i=1}^N g(\mathbf{x}^i)^2, \quad \mathbf{x}^i \in \Gamma \subset \partial\Omega, \quad i = 1, \dots, N. \quad (41)$$

The root mean square errors for the internal temperature, $\text{Err}_{\Omega}(u)$, and normal heat flux on the boundary, $\text{Err}_{\Gamma}(\phi)$, can be defined in a similar manner.

The root mean square errors for the boundary temperature, $\text{Err}_{\Gamma}(u)$, $\Gamma = \partial\Omega \setminus \Gamma_D$, normal heat flux

on the boundary $\Gamma = \partial\Omega \setminus \Gamma_N$, $\text{Err}_{\Gamma}(\phi)$, and internal temperature, $\text{Err}_{\Omega}(u)$, as functions of the truncation number n_{SVD} , obtained for various levels of noise, p_u , added into the Dirichlet data, in the case of Formulation 1 for the Example 1, are shown in Figs. 4(a), (b) and (c), respectively. From these figures it can be seen that the accuracy errors $\text{Err}_{\Gamma}(u)$, $\text{Err}_{\Gamma}(\phi)$ and $\text{Err}_{\Omega}(u)$ decrease as the amount of noise, p_u , decreases for all the values of the truncation number. Moreover, for a given level of noise, p_u , these errors satisfy the following inequality $\text{Err}_{\Omega}(u) < \text{Err}_{\Gamma}(u) < \text{Err}_{\Gamma}(\phi)$, for all the values of the truncation number, n_{SVD} , i.e. the inaccuracies in the numerical normal heat flux on the boundary $\partial\Omega \setminus \Gamma_N$ are larger than those corresponding to the temperature on the boundary $\partial\Omega \setminus \Gamma_D$, which are larger than the inaccuracies in the numerical results for the internal temperature. Furthermore, by comparing Figs. 3 and 4, it can be seen that the corner of the L-curves occurs at about the same value of the truncation number n_{SVD} where the minimum in the root mean square errors $\text{Err}_{\Gamma}(u)$, $\text{Err}_{\Gamma}(\phi)$ and $\text{Err}_{\Omega}(u)$ is attained. Hence we may conclude that the L-curve criterion provides a very good tool to determine the optimal value of the regularization parameter, i.e. the optimal truncation number for the SVD.



(a)

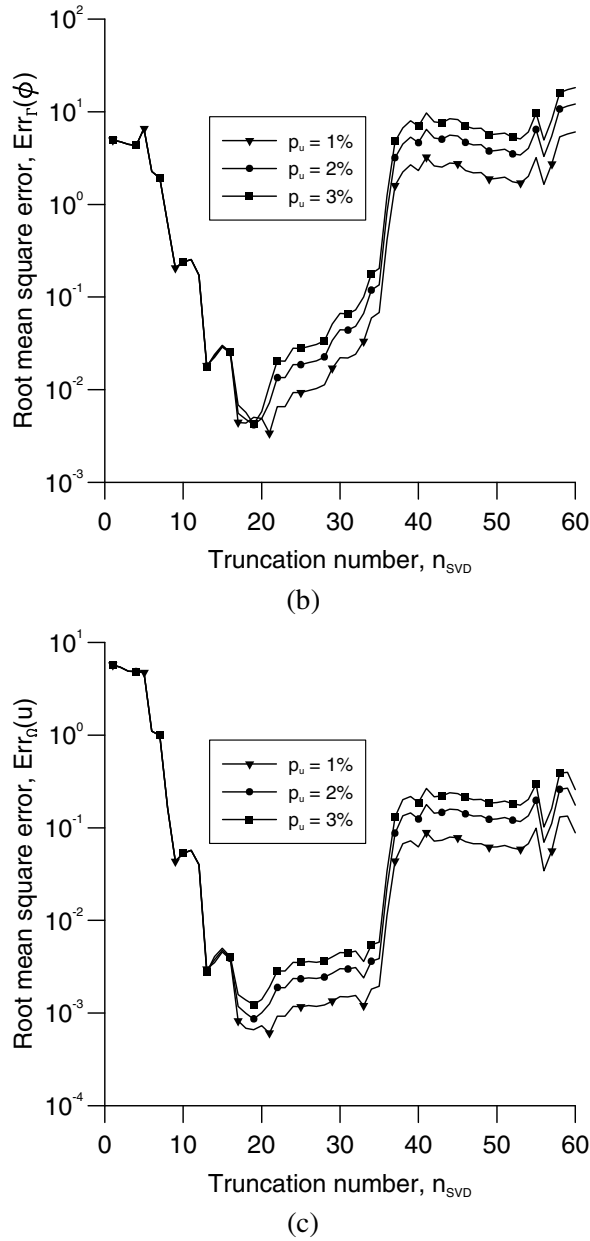


Figure 4: The root mean square errors (a) $\text{Err}_{\Gamma}(u)$, $\Gamma = \partial\Omega \setminus \Gamma_D$, (b) $\text{Err}_{\Gamma}(\phi)$, $\Gamma = \partial\Omega \setminus \Gamma_N$, and (c) $\text{Err}_{\Omega}(u)$, as functions of the truncation number n_{SVD} , obtained using $n_D = n_N = 30$ boundary collocation points, $n_{\text{int}} = 0$ internal collocation points and $n_s = 60$ singularities for the homogeneous solution u_h , and various levels of noise added into the Dirichlet boundary data $\tilde{u}|_{\Gamma_D}$, namely $p_u \in \{1\%, 2\%, 3\%\}$, in the case of Formulation 1 for Example 1.

5.4 Stability of the method

Figs. 5(a) and (b) illustrate the analytical and numerical results for the boundary temperature $u|_{\partial\Omega \setminus \Gamma_D}$ and normal heat flux $\phi|_{\partial\Omega \setminus \Gamma_N}$, respectively, obtained using the optimal truncation number n_{SVD} chosen according to the L-curve criterion, $n_D = n_N = 30$ boundary collocation points, $n_{\text{int}} = 0$ internal collocation points and $n_s = 60$ singularities for approximating the solution of the homogeneous problem (7.1) – (7.4), and various levels of noise added into the Dirichlet boundary data $\tilde{u}|_{\Gamma_D}$, namely $p_u \in \{1\%, 2\%, 3\%\}$, in the case of Formulation 1 for Example 1. From these figures we can conclude that the numerical solutions retrieved in the case of Formulation 1 for Example 1 are stable with respect to decreasing the amount of noise added into the boundary temperature $\tilde{u}|_{\Gamma_D}$ and hence the L-curve method has a stabilizing character.

A similar conclusion can be drawn from Fig. 6(a), which presents the numerical results for the boundary temperature $u|_{\partial\Omega}$, obtained using the optimal truncation number n_{SVD} chosen according to the L-curve criterion, $n_D = 0$ and $n_N = 40$ boundary collocation points, $n_{\text{int}} = 40$ internal collocation points and $n_s = 60$ singularities for the homogeneous solution u_h , and various levels of noise added into the internal temperature data $\tilde{u}|_{\Omega_{\text{int}}}$, namely $p_u \in \{1\%, 2\%, 3\%\}$, in the case of Formulation 3 for Example 1, in comparison with its corresponding analytical values. These stability results are better emphasized in Fig. 6(b) that shows the percentage normalised errors, $\text{err}_{\Gamma}(u)$, associated with the numerical results retrieved for the inverse problem mentioned above, defined as

$$\text{err}_{\Gamma}(u(\mathbf{x})) = \frac{|u^{(\text{an})}(\mathbf{x}) - u^{(\text{num})}(\mathbf{x})|}{\max_{\mathbf{y} \in \partial\Omega} |u^{(\text{an})}(\mathbf{y})|} \times 100, \mathbf{x} \in \partial\Omega. \quad (42)$$

The values of the optimal truncation number, n_{SVD} , obtained according to the L-curve criterion, and the numerical results, retrieved using various levels of noisy boundary and internal temperature data in the case of Formulations 1 and 3, respectively, are presented in Tab. 1 in terms of the accuracy errors $\text{Err}_{\Gamma}(u)$, $\text{Err}_{\Gamma}(\phi)$ and $\text{Err}_{\Omega}(u)$. From

Table 1: The accuracy errors, $\text{Err}_\Gamma(u)$ ($\Gamma = \partial\Omega \setminus \Gamma_D$), $\text{Err}_\Gamma(\phi)$ ($\Gamma = \partial\Omega \setminus \Gamma_N$) and $\text{Err}_\Omega(u)$, and the values of the optimal truncation number, n_{SVD} , obtained using several amounts of noise added into the boundary or internal data, for the inverse problems investigated.

Example	Formulation	$p_u _\Gamma$	$p_\phi _\Gamma$	$p_u _{\Omega_{\text{int}}}$	n_{SVD}	$\text{Err}_\Gamma(u)$	$\text{Err}_\Gamma(\phi)$	$\text{Err}_\Omega(u)$
1	1	1%	0%	0%	18	3.82×10^{-3}	3.36×10^{-3}	6.82×10^{-4}
		2%	0%	0%	19	4.34×10^{-3}	4.16×10^{-3}	8.63×10^{-4}
		3%	0%	0%	19	5.56×10^{-3}	4.23×10^{-3}	1.23×10^{-3}
	3	0%	0%	1%	21	2.63×10^{-5}	1.56×10^{-4}	3.05×10^{-6}
		0%	0%	2%	21	5.25×10^{-5}	1.96×10^{-4}	6.09×10^{-6}
		0%	0%	3%	21	7.87×10^{-5}	5.49×10^{-4}	9.12×10^{-6}
2	2	1%	0%	0%	14	1.76×10^{-3}	2.61×10^{-3}	1.19×10^{-4}
		2%	0%	0%	14	2.49×10^{-3}	3.34×10^{-3}	2.10×10^{-4}
		3%	0%	0%	14	3.26×10^{-3}	4.21×10^{-3}	3.04×10^{-4}
3	1	0%	1%	0%	17	2.06×10^{-4}	5.03×10^{-4}	4.28×10^{-5}
		0%	2%	0%	17	4.17×10^{-4}	9.86×10^{-4}	8.70×10^{-5}
		0%	3%	0%	17	6.27×10^{-4}	1.46×10^{-3}	1.31×10^{-4}

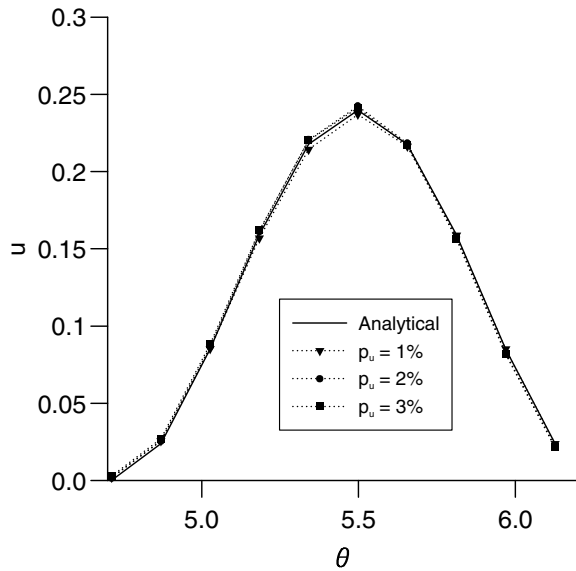
this table, as well as Figs. 5 and 6, it can be seen that, as expected, the numerical results obtained using noisy boundary temperature data are more inaccurate than those retrieved with noisy internal temperature data, for the same amount of noise added into the temperature measurements.

Further, we investigate the stability of the proposed numerical method for the inverse problem (3.1) – (3.4) in the piecewise smooth, simply connected, two-dimensional domain considered in Example 2, i.e. the square $\Omega = (-0.5, 0.5)^2$. The analytical and numerical results for the unknown temperature and normal heat flux on the boundary $\{-0.5\} \times [-0.5, 0.5]$, obtained using the optimal truncation number n_{SVD} chosen according to the L-curve criterion, various amounts of noise added into the temperature $\tilde{u}|_{\Gamma_D}$, namely $p_u \in \{1\%, 2\%, 3\%\}$, in the case of Formulation 2 for Example 2, are presented in Fig. 7. The corresponding root mean square errors $\text{Err}_\Gamma(u)$, $\text{Err}_\Gamma(\phi)$ and $\text{Err}_\Omega(u)$ are also tabulated in Tab. 1. From Fig. 7, as well as Tab. 1, we can conclude that the proposed numerical method, in conjunction with the L-curve criterion, also provides stable and accurate numerical results for inverse problems in piecewise smooth, simply connected, two-dimensional domains.

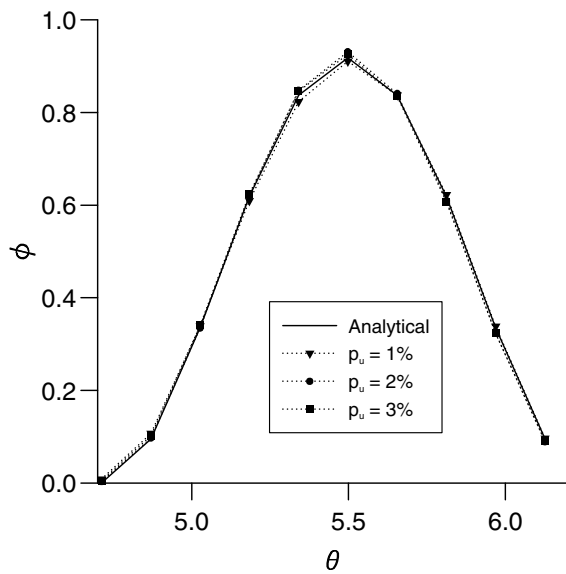
The MFS+SVD algorithm works equally well when solving the inverse problem (3.1) – (3.4) in a smooth, doubly connected, two-dimensional domain, such as the annular domain considered in Example 3. Figs. 8(a) and (b) show the same accurate and stable numerical results for the unknown boundary temperature $u|_{\partial\Omega \setminus \Gamma_D}$ and normal heat flux $\phi|_{\partial\Omega \setminus \Gamma_N}$, respectively, obtained in the case of Formulation 1 for Example 3, using the optimal truncation number n_{SVD} chosen according to the L-curve criterion, $n_D = n_N = 40$ boundary collocation points, $n_{\text{int}} = 0$ internal collocation points and $n_s = 40$ singularities for the homogeneous solution u_h , and various levels of noise added into the Neumann boundary data $\tilde{\phi}|_{\Gamma_N}$, namely $p_\phi \in \{1\%, 2\%, 3\%\}$. From the numerical results presented in this section, illustrated in Figs. 5 – 8 and tabulated in Tab. 1, we can conclude that the proposed MFS+SVD algorithm is stable with respect to decreasing the amount of noise added into the boundary and/or internal data, whilst the L-curve method employed for choosing the optimal value for the truncation number n_{SVD} has a regularizing character.

5.5 Convergence of the method

Based on the numerical examples analysed in this paper, we investigate the convergence of the pro-

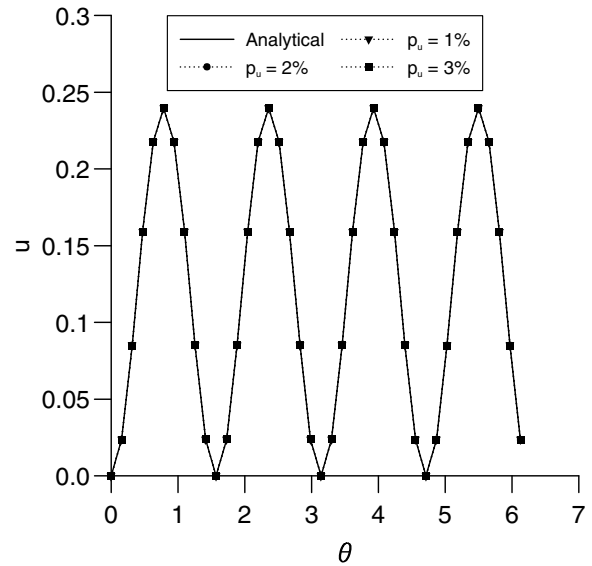


(a)

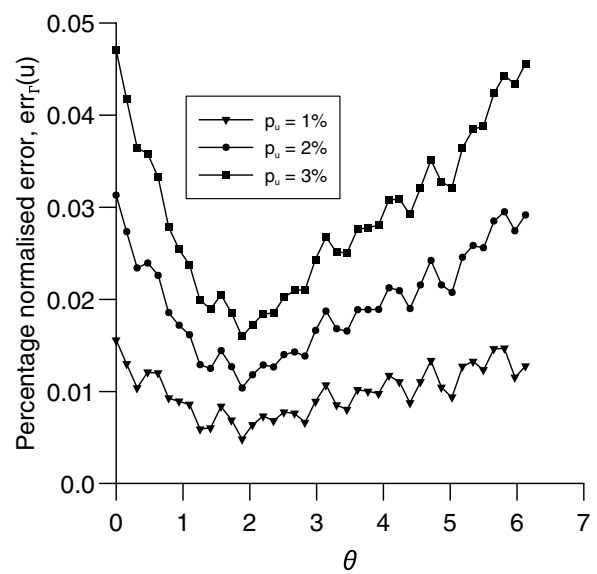


(b)

Figure 5: The analytical (—) and the numerical values for (a) the temperature u on the boundary $\partial\Omega \setminus \Gamma_D$, and (b) the normal heat flux ϕ on the boundary $\partial\Omega \setminus \Gamma_N$, obtained using $n_D = n_N = 30$ boundary collocation points, $n_{\text{int}} = 0$ internal collocation points and $n_s = 60$ singularities for the homogeneous solution u_h , and various levels of noise added into the Dirichlet boundary data $\tilde{u}|_{\Gamma_D}$, namely $p_u = 1\%$ ($\cdots \blacktriangledown \cdots$), $p_u = 2\%$ ($\cdots \bullet \cdots$) and $p_u = 3\%$ ($\cdots \blacksquare \cdots$), in the case of Formulation 1 for Example 1.

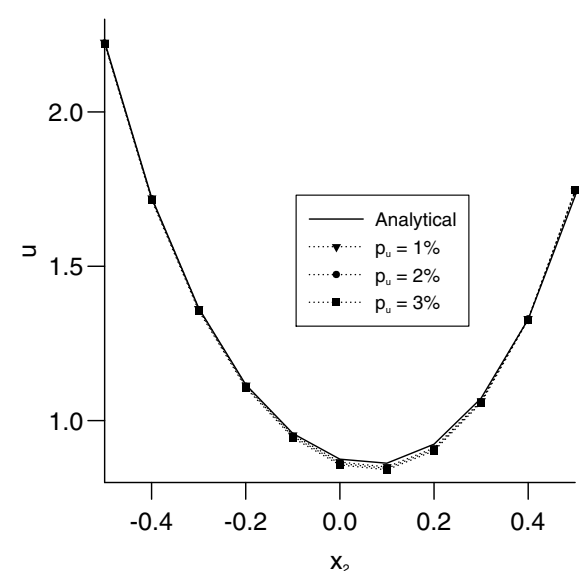


(a)

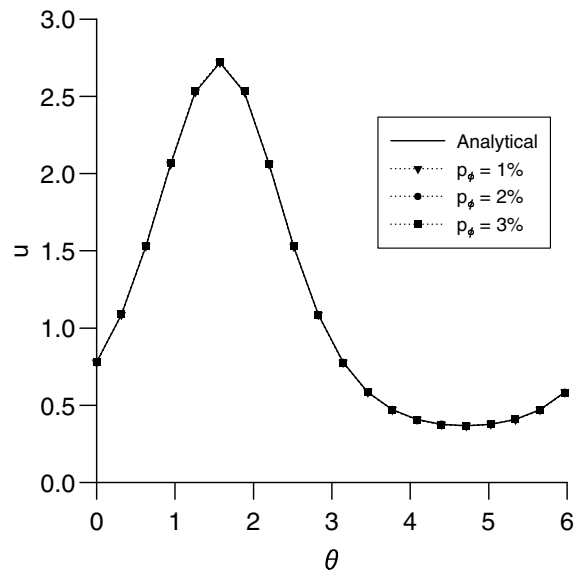


(b)

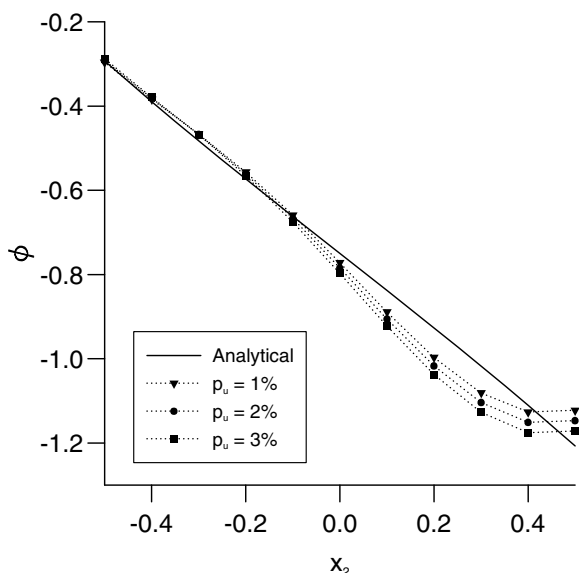
Figure 6: The analytical (—) and the numerical values for (a) the temperature u on the boundary $\partial\Omega$, and (b) the percentage normalised error, $\text{err}_{\Gamma}(u)$, obtained using $n_D = 0$ and $n_N = 40$ boundary collocation points, $n_{\text{int}} = 40$ internal collocation points and $n_s = 60$ singularities for the homogeneous solution u_h , and various levels of noise added into the internal temperature data $\tilde{u}|_{\Omega_{\text{int}}}$, namely $p_u = 1\%$ ($\cdots \blacktriangledown \cdots$), $p_u = 2\%$ ($\cdots \bullet \cdots$) and $p_u = 3\%$ ($\cdots \blacksquare \cdots$), in the case of Formulation 3 for Example 1.



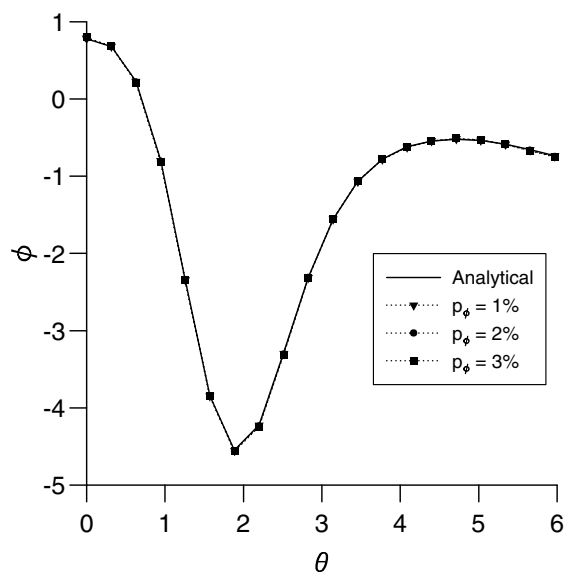
(a)



(a)



(b)



(b)

Figure 7: The analytical (—) and the numerical values for (a) the temperature u , and (b) the normal heat flux ϕ , on the boundary $\{-0.5\} \times [-0.5, 0.5]$, obtained using $n_D = 30$ and $n_N = 20$ boundary collocation points, $n_{\text{int}} = 0$ internal collocation points and $n_s = 40$ singularities for the homogeneous solution u_h , and various levels of noise added into the Dirichlet data $\tilde{u}|_{\Gamma_D}$, namely $p_u = 1\%$ ($\cdots \blacktriangledown \cdots$), $p_u = 2\%$ ($\cdots \bullet \cdots$) and $p_u = 3\%$ ($\cdots \blacksquare \cdots$), in the case of Formulation 2 for Example 2.

Figure 8: The analytical (—) and the numerical values for (a) the temperature u on the boundary $\partial\Omega \setminus \Gamma_D$, and (b) the normal heat flux ϕ on the boundary $\partial\Omega \setminus \Gamma_N$, obtained using $n_D = n_N = 40$ boundary collocation points, $n_{\text{int}} = 0$ internal collocation points and $n_s = 40$ singularities for the homogeneous solution u_h , and various levels of noise added into the Neumann boundary data $\tilde{\phi}|_{\Gamma_N}$, namely $p_\phi = 1\%$ ($\cdots \blacktriangledown \cdots$), $p_\phi = 2\%$ ($\cdots \bullet \cdots$) and $p_\phi = 3\%$ ($\cdots \blacksquare \cdots$), in the case of Formulation 1 for Example 3.

posed method with respect to the number of singularities, n_s , and the distance, d_s , between the source points and the boundary of the solution domain. To do so, we consider the inverse problem (3.1) – (3.4) in the case of Formulation 1 for Example 3, see Eqs. (35) – (38).

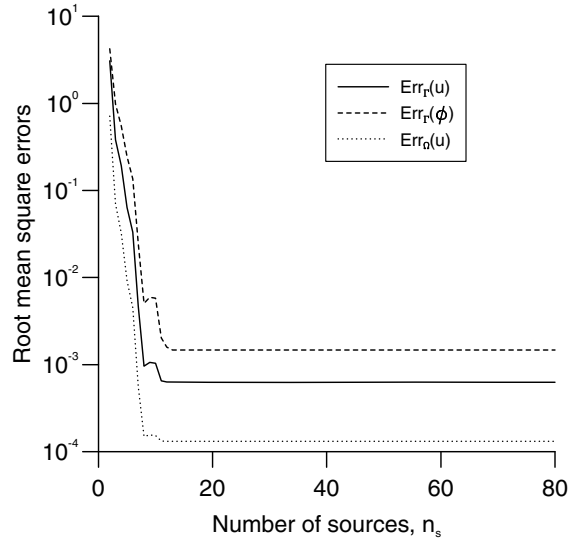


Figure 9: The root mean square errors $\text{Err}_\Gamma(u)$ (—), $\Gamma = \partial\Omega \setminus \Gamma_D$, $\text{Err}_\Gamma(\phi)$ (---), $\Gamma = \partial\Omega \setminus \Gamma_N$, and $\text{Err}_\Omega(u)$ (⋯), as functions of the number of singularities n_s , obtained using $n_D = n_N = 40$ boundary collocation points and $n_{\text{int}} = 0$ internal collocation points for the homogeneous solution u_h , and $p_\phi = 3\%$ noise added into the Neumann boundary data $\tilde{\phi}|_{\Gamma_N}$, in the case of Formulation 1 for Example 3.

The numerical results obtained using $n_D = n_N = 40$ boundary collocation points and $n_{\text{int}} = 0$ internal collocation points for the homogeneous solution u_h , and $p_\phi = 3\%$ noise added into the Neumann boundary data $\tilde{\phi}|_{\Gamma_N}$, are presented in Fig. 9 in terms of the accuracy errors $\text{Err}_\Gamma(u)$, $\text{Err}_\Gamma(\phi)$ and $\text{Err}_\Omega(u)$, as functions of the number of sources $n_s \in \{1, 2, \dots, 80\}$. Although not presented here, it is reported that similar results have been obtained for the other inverse problems investigated in this study. From Fig. 9 it can be seen that the root mean square errors $\text{Err}_\Gamma(u)$, $\text{Err}_\Gamma(\phi)$ and $\text{Err}_\Omega(u)$ decrease until the number of singu-

larities reaches the value $n_s = 10$, after which a further increase in the number of singularities, n_s , does not improve substantially the accuracy of the numerical results. The numerical results are practically the same for $n_s \geq 10$ in the case of Formulation 1 for Example 3 and this indicates that accurate numerical results for the unknown boundary temperature and normal heat flux, as well as the unknown internal temperature, can be obtained using a relatively small number of singularities. Furthermore, from Fig. 9 we can also conclude that the proposed MFS+SVD algorithm is convergent with respect to increasing the number of singularities, n_s .

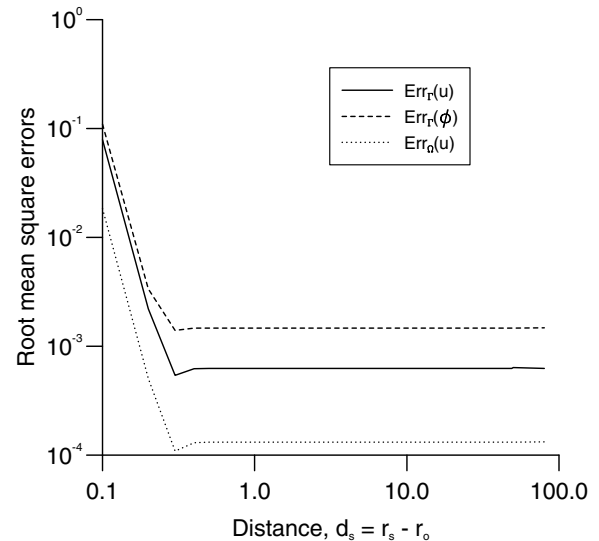


Figure 10: The root mean square errors $\text{Err}_\Gamma(u)$ (—), $\Gamma = \partial\Omega \setminus \Gamma_D$, $\text{Err}_\Gamma(\phi)$ (---), $\Gamma = \partial\Omega \setminus \Gamma_N$, and $\text{Err}_\Omega(u)$ (⋯), as functions of the distance between the singularities and the boundary of the solution domain, $d_s = r_s - r_o$, obtained using $n_D = n_N = 40$ boundary collocation points, $n_{\text{int}} = 0$ internal collocation points and $n_s = 40$ singularities for the homogeneous solution u_h , and $p_\phi = 3\%$ noise added into the Neumann boundary data $\tilde{\phi}|_{\Gamma_N}$, in the case of Formulation 1 for Example 3.

It is well-known that the accuracy of the MFS depends on the distance, d_s , between the pseudo-boundary on which the singularities are located and the boundary of the solution domain. For di-

rect problems with exact data, it is generally advised to place the singularities as far away from the boundary of the domain under investigation as possible, as much as the machine precision allows. Ramachandran (2002) showed that the SVD could mitigate this critical dependence, which is also the case for direct problems with noisy data, see e.g. Jin (2005). The root mean square errors $\text{Err}_\Gamma(u)$, $\text{Err}_\Gamma(\phi)$ and $\text{Err}_\Omega(u)$ as functions of the distance, $0.1 \leq d_s = r_s - r_o \leq 100$, between the singularities and the boundary $\partial\Omega$, obtained using $n_D = n_N = 40$ boundary collocation points, $n_{\text{int}} = 0$ internal collocation points and $n_s = 40$ singularities for the homogeneous solution u_h , and $p_\phi = 3\%$ noise added into the Neumann boundary data $\tilde{\phi}|_{\Gamma_N}$, in the case of Formulation 1 for Example 3, are presented in Fig. 10. It can be seen from this figure that the accuracy of the numerical results improves as the distance, d_s between the singularities and the boundary $\partial\Omega$ increases. In addition, the accuracy errors $\text{Err}_\Gamma(u)$, $\text{Err}_\Gamma(\phi)$ and $\text{Err}_\Omega(u)$ obtained using the MFS+SVD algorithm are reasonable even when the singularities are located very close to the boundary $\partial\Omega$, whilst the accuracy in the numerical results for the boundary temperature and normal heat flux, as well as the internal temperature, does not improve significantly for $0.5 \leq d_s \leq 100.0$ and is relatively independent of the distance d_s . It is interesting to note that the numerical results obtained for the unknown boundary and internal temperatures and the normal heat flux using very large values of d_s , for example $d_s = 1.0 \times 10^5$, are still in excellent agreement with their corresponding analytical values. A similar phenomenon has been observed for the other examples and formulations investigated in this study. This is a remarkable result since it is in accordance with the theoretical results, see e.g. Golberg and Chen (1999), and Fairweather and Karageorghis (1998), and contrary to the findings in the case of the MFS applied in conjunction with the Tikhonov regularization method to solve inverse problems associated with the steady-state heat conduction in functionally graded materials, see e.g. Marin (2005b). Overall, from Figs. 9 and 10 we can conclude that the proposed numerical method is convergent with respect to increasing both the number of sin-

gularities and the distance between the singularities and the boundary of the solution domain.

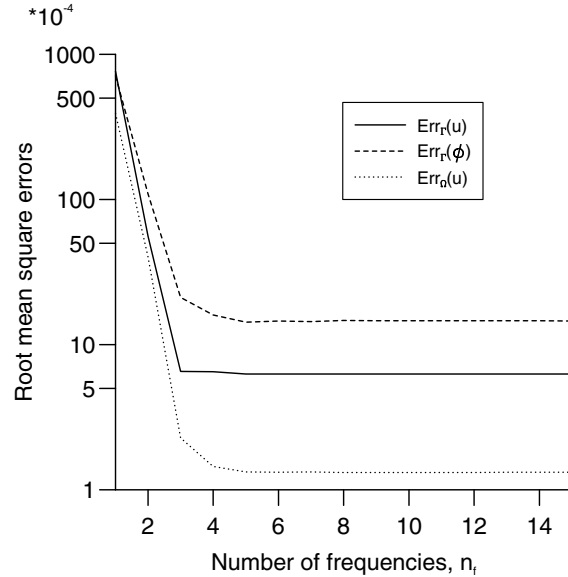


Figure 11: The root mean square errors $\text{Err}_\Gamma(u)$ (—), $\Gamma = \partial\Omega \setminus \Gamma_D$, $\text{Err}_\Gamma(\phi)$ (---), $\Gamma = \partial\Omega \setminus \Gamma_N$, and $\text{Err}_\Omega(u)$ (···), as functions of the number of frequencies n_f , obtained using $n_D = n_N = 40$ boundary collocation points, $n_{\text{int}} = 0$ internal collocation points and $n_s = 40$ singularities for the homogeneous solution u_h , and $p_\phi = 3\%$ noise added into the Neumann boundary data $\tilde{\phi}|_{\Gamma_N}$, in the case of Formulation 1 for Example 3.

5.6 Sensitivity analysis

It is the purpose of this section to investigate the influence of the number n_f of frequencies λ_k , $k = 1, \dots, n_f$, used to approximate the particular solution u_p on the numerical results obtained with the MFS+SVD algorithm. To do so, we consider Formulation 1 for Example 3, and set $n_D = n_N = 40$ boundary collocation points, $n_{\text{int}} = 0$ internal collocation points and $n_s = 40$ singularities for the homogeneous solution u_h , $n_{\text{dc}} = 400$ domain collocation points and $n_{\text{ds}} = 16$ source points for the particular solution u_p , and $p_\phi = 3\%$ noise added into the Neumann boundary data $\tilde{\phi}|_{\Gamma_N}$, while at the same time we vary the number of frequencies n_f . Fig. 10 illustrates the root mean square

errors $\text{Err}_\Gamma(u)$, $\text{Err}_\Gamma(\phi)$ and $\text{Err}_\Omega(u)$ retrieved using various numbers of frequencies, namely $n_f \in \{1, 2, \dots, 15\}$. It should be mentioned that a very low number of frequencies, λ_k , $k = 1, \dots, n_f$, used for approximating the right-hand side of Eq. (5), e.g. $n_f \in \{1, 2, 3\}$, implies a very poor approximation for the particular solution u_p . This gives rise to a very high level of noise added into the boundary and internal data (in addition to the perturbations of the exact boundary and/or internal data due to the inaccuracies in the boundary and/or internal measurements) for the homogeneous problem (7.1) – (7.4) associated with the inverse problem (3.1) – (3.4), which can be clearly observed from the results presented in Fig. 11. However, it can be seen from this figure that the accuracy errors $\text{Err}_\Gamma(u)$, $\text{Err}_\Gamma(\phi)$ and $\text{Err}_\Omega(u)$ follow a similar pattern and they all reach a plateau region for $n_f \geq 4$. Therefore, only a small number of frequencies λ_k , $k = 1, \dots, n_f$, i.e. $n_f = 4$, is sufficient for obtaining a satisfactory approximation of the particular solution u_p and hence very accurate numerical results for the unknown boundary and internal temperature, and boundary normal heat flux. Similar results have been obtained for the other formulations and examples considered in this study, which are therefore omitted.

6 Conclusions

In this paper, a numerical scheme for solving inverse boundary value problems associated with the steady-state heat conduction in isotropic media in the presence of sources was proposed. The present numerical procedure is based on the MFS and requires the approximation of a particular solution to an inhomogeneous equation (Poisson equation) and the numerical solution of the associated inverse boundary value problem for a homogeneous equation (Laplace equation). The particular solution is approximated based on the method proposed by Alves and Chen (2005), whilst the homogeneous solution is obtained by applying the classical MFS. Since the inverse problems under consideration are ill-conditioned, they have been regularized by employing the SVD, whilst the optimal regularization parameter, namely the optimal SVD trun-

cation number, was chosen according to the L-curve criterion. The inverse boundary value problems analysed in this study have been solved in smooth and piecewise smooth, simply and doubly connected, two-dimensional domains, whilst three possible formulations of the problem, which account for incomplete boundary normal heat flux measurements and additional internal or boundary temperature measurements, have been considered. The numerical results obtained show that the proposed numerical method is efficient, accurate, convergent and stable, and represents a competitive alternative to existing methods used for solving inverse boundary value problems associated with the steady-state heat conduction in isotropic media in the presence of sources. Furthermore, the MFS+SVD algorithm is easy to adapt to inverse problems for the Poisson equation in domains with boundary singularities, such as L-shaped domains, domains with V-notches, boundary cracks etc, and three-dimensional geometries, as well as other inhomogeneous linear partial differential equations, such as the steady-state heat conduction in anisotropic media in the presence of sources. However, these are deferred to future work.

References

- Alves, C.J.S.; Chen, C.S.** (2005): A new method of fundamental solutions applied to nonhomogeneous elliptic problems. *Advances in Computational Mathematics*, vol. 23, pp. 125–142.
- Balakrishnan, K.; Ramachandran, P.A.** (1999): A particular solution Trefftz method for nonlinear Poisson problems in heat and mass transfer. *Journal of Computational Physics*, vol. 150, pp. 239–267.
- Beck, J.V.; Blackwell, B.; St. Clair, C.R.** (1985): *Inverse Heat Conduction: Ill-Posed Problems*, Wiley-Interscience, New York.
- Berger, J.R.; Karageorghis, A.** (1999): The method of fundamental solutions for heat conduction in layered materials. *International Journal for Numerical Methods in Engineering*, vol. 45, pp. 1681–1694.
- Berger, J.R.; Karageorghis, A.** (2001): The

method of fundamental solutions for layered elastic materials. *Engineering with Analysis Boundary Elements*, vol. 25, pp. 877–886.

Castellanos, J.L.; Gomez, S.; Guerra, V. (2002): The triangle method for finding the corner of the L-curve. *Applied Numerical Mathematics*, vol. 43, pp. 359–373.

Chao, R.-M.; Chen, Y.-J.; Lin, F.C. (2001): Determining the unknown traction of a cracked elastic body using the inverse technique with the dual boundary element method. *CMES: Computer Modeling in Engineering & Sciences*, vol. 2, pp. 73–86.

Chen, C.S.; Cho, H.A.; Golberg, M.A. (2006): Some comments on the ill-conditioning of the method of fundamental solutions. *Engineering with Analysis Boundary Elements*, vol. 30, pp. 405–410.

Chen, L.Y.; Chen, J.T.; Hong, H.K.; Chen, C.H. (1995): Application of Cesàro mean and the L-curve for the deconvolution problem, *Soil Dynamics Earthquake Engineering*, vol. 14, pp. 361–373.

de Lacerda, L.A.; da Silva, J.M. (2006): A dual BEM genetic algorithm scheme for the identification of polarization curves of buried slender structures. *CMES: Computer Modeling in Engineering & Sciences*, vol. 14, pp. 153–160.

Fairweather, G.; Karageorghis, A. (1998): The method of fundamental solutions for elliptic boundary value problems. *Advances in Computational Mathematics*, vol. 9, pp. 69–95.

Golberg, M.A. (1995): The numerical evaluation of particular solutions in BEM - A review, *Boundary Element Communications*, vol. 6, pp. 99–106.

Golberg, M.A.; Chen, C.S. (1994): The theory of radial basis functions. *Boundary Element Communications*, vol. 5, pp. 57–61.

Golberg, M.A.; Chen, C.S. (1996): *Discrete Projection Methods for Integral Equations*, Computational Mechanics Publications, Southampton.

Golberg, M.A.; Chen, C.S. (1999): The method of fundamental solutions for potential, Helmholtz and diffusion problems. In: M.A. Golberg (ed.) *Boundary Integral Methods: Numerical and*

Mathematical Aspects, WIT Press and Computational Mechanics Publications, Boston, pp. 105–176.

Guerra, V.; Hernandez, V. (2001): Numerical aspects in locating the corner of the L-curve. In: M. Lassonde (ed.) *Approximation, Optimization and Mathematical Economics*, Springer-Verlag, Heidelberg, pp. 121–131.

Hadamard, J. (1923): *Lectures on Cauchy Problem in Linear Partial Differential Equations*, Oxford University Press, London.

Hanke, M. (1996): Limitations of the L-curve method in ill-posed problems. *BIT*, vol. 36, pp. 287–301.

Hansen, P.C. (1998): *Rank-Deficient and Discrete Ill-Posed Problems: Numerical Aspects of Linear Inversion*, SIAM, Philadelphia.

Hansen, P.C. (2001): The L-curve and its use in the numerical treatment of inverse problems. In: P. Johnston (ed.) *Computational Inverse Problems in Electrocardiology*, WIT Press, Southampton, pp. 119–142.

Hào, D.N.; Lesnic, D. (2000): The Cauchy problem for Laplace's equation via the conjugate gradient method. *IMA Journal of Applied Mathematics*, vol. 65, pp. 199–217.

Harris, S.D.; Mustata, R.; Elliott, L.; Ingham, D.B.; Lesnic, D. (2008): Numerical identification of the hydraulic conductivity of composite anisotropic materials. *CMES: Computer Modeling in Engineering & Sciences*, vol. 25, pp. 69–79.

Hon, Y.C.; Wei, T. (2004): A fundamental solution method for inverse heat conduction problems. *Engineering with Analysis Boundary Elements*, vol. 28, pp. 489–495.

Huang, C.-H.; Shih, C.-C. (2007): An inverse problem in estimating simultaneously the time-dependent applied force and moment of an Euler-Bernoulli beam. *CMES: Computer Modeling in Engineering & Sciences*, vol. 21, pp. 239–254.

Ingham, D.B.; Yuan, Y. (1994): Boundary element solutions of the steady state, singular, inverse heat transfer equation, *International Journal of Heat and Mass Transfer*, vol. 37, pp. 273–

280.

Jin, B.T. (2005): A meshless method for the Laplace and biharmonic equations subjected to noisy data. *CMES: Computer Modeling in Engineering & Sciences*, vol. 6, pp. 253–261.

Jin, B.T.; Marin, L. (2007): The method of fundamental solutions for inverse source problems associated with the steady-state heat conduction. *International Journal for Numerical Methods in Engineering*, vol. 69, pp. 1570–1589.

Jin, B.T.; Zheng, Y. (2006): A meshless method for some inverse problems associated with the Helmholtz equation. *Computer Methods in Applied Mechanics and Engineering*, vol. 195, pp. 2270–2280.

Karageorghis, A.; Fairweather, G. (1987): The method of fundamental solutions for the numerical solution of the biharmonic equation. *Journal of Computational Physics*, vol. 69, pp. 434–459.

Karageorghis, A.; Fairweather, G. (2000): The method of fundamental solutions for axisymmetric elasticity problems. *Computational Mechanics*, vol. 25, pp. 524–532.

Kaufman, L.; Neumaier, A. (1996): PET regularization by envelope guided conjugate gradients, *IEEE Transactions on Medical Imaging*, vol. 15, pp. 385–389.

Kraus, A.D.; Aziz, A.; Welty, J. (2001): *Extended Surface Heat Transfer*, Wiley-Interscience, New York.

Kress, R. (1989): *Linear Integral Equations*, Springer-Verlag, Berlin.

Kupradze, V.D.; Aleksidze, M.A. (1964): The method of functional equations for the approximate solution of certain boundary value problems. *USSR Computational Mathematics and Mathematical Physics*, vol. 4, pp. 82–126.

Lesnic, D.; Elliott, L.; Ingham, D.B. (1997): An iterative boundary element method for solving numerically the Cauchy problem for the Laplace equation. *Engineering with Analysis Boundary Elements*, vol. 20, pp. 123–133.

Lesnic, D.; Elliott, L.; Ingham, D.B. (1998): The solution of an inverse heat conduction problem subject to the specification of energies. *Inter-*

national Journal of Heat and Mass Transfer, vol. 41, pp. 25–32.

Ling, X.; Atluri, S.N. (2006): Stability analysis for inverse heat conduction problems. *CMES: Computer Modeling in Engineering & Sciences*, vol. 13, pp. 219–228.

Liu, C.-S. (2006): An efficient simultaneous estimation of temperature-dependent thermophysical properties. *CMES: Computer Modeling in Engineering & Sciences*, vol. 14, pp. 77–90.

Liu, C.-S.; Liu, L.-W.; Hong, H.-K. (2007): Highly accurate computation of spatial-dependent heat conductivity and heat capacity in inverse thermal problem. *CMES: Computer Modeling in Engineering & Sciences*, vol. 17, pp. 1–18.

Marin, L. (2005a): A meshless method for solving the Cauchy problem in three-dimensional elastostatics. *Computers & Mathematics with Applications*, vol. 50, pp. 73–92.

Marin, L. (2005b): Numerical solutions of the Cauchy problem for steady-state heat transfer in two-dimensional functionally graded materials. *International Journal of Solids and Structures*, vol. 42, pp. 4338–4351.

Marin, L. (2005c): A meshless method for the numerical solution of the Cauchy problem associated with three-dimensional Helmholtz-type equations. *Applied Mathematics and Computation*, vol. 165, pp. 355–374.

Marin, L.; Lesnic, D. (2004): The method of fundamental solutions for the Cauchy problem in two-dimensional linear elasticity. *International Journal of Solids and Structures*, vol. 41, pp. 3425–3438.

Marin, L.; Lesnic, D. (2005): The method of fundamental solutions for the Cauchy problem associated with two-dimensional Helmholtz-type equations, *Computers & Structures*, vol. 83, pp. 267–278.

Marin, L.; Elliott, L.; Ingham, D.B.; Lesnic, D. (2001): Boundary element method for the Cauchy problem in linear elasticity. *Engineering Analysis with Boundary Elements*, vol. 25, pp. 783–793.

Marin, L.; Elliott, L.; Ingham, D.B.; Lesnic, D. (2002): Boundary element regularization meth-

ods for solving the Cauchy problem in linear elasticity. *Inverse Problems in Engineering*, vol. 10, pp. 335–357.

Marin, L.; Heggs, P.J.; Elliott, L.; Ingham, D.B.; Lesnic, D.; Wen, X. (2003a): An alternating iterative algorithm for the Cauchy problem associated to the Helmholtz equation. *Computer Methods in Applied Mechanics and Engineering*, vol. 192, pp. 709–722.

Marin, L.; Heggs, P.J.; Elliott, L.; Ingham, D.B.; Lesnic, D.; Wen, X. (2003b): Conjugate gradient-boundary element solution to the Cauchy problem for Helmholtz-type equations. *Computational Mechanics*, vol. 31, pp. 367–377.

Marin, L.; Heggs, P.J.; Elliott, L.; Ingham, D.B.; Lesnic, D.; Wen, X. (2004): BEM solution for the Cauchy problem associated with Helmholtz-type equations by the Landweber method, *Engineering with Analysis Boundary Elements*, vol. 28, pp. 1025–1034.

Marin, L.; Power, H.; Bowtell, R.W.; Sanchez, C.C.; Becker, A.A.; Glover, P.; Jones, A. (2008): Boundary element method for an inverse problem in magnetic resonance imaging gradient coils. *CMES: Computer Modeling in Engineering & Sciences*, vol. 23, pp. 149–174.

Mathon, R.; Johnston, R.L. (1977): The approximate solution of elliptic boundary value problems by fundamental solutions. *SIAM Journal on Numerical Analysis*, vol. 14, pp. 638–650.

Mera, N.S. (2005): The method of fundamental solutions for the backward heat conduction problem. *Inverse Problems in Science and Engineering*, vol. 13, pp. 79–98.

Mera, N.S.; Elliott, L.; Ingham, D.B. (2006): The detection of super-elliptical inclusions in infrared computerised axial tomography. *CMES: Computer Modeling in Engineering & Sciences*, vol. 15, pp. 107–114.

Mera, N.S.; Elliott, L.; Ingham, D.B.; Lesnic, D. (2000): The boundary element solution of the Cauchy steady state heat conduction problem in an anisotropic medium. *International Journal for Numerical Methods in Engineering*, vol. 49, pp. 481–499.

Mera, N.S.; Elliott, L.; Ingham, D.B.; Lesnic,

D. (2002): The boundary element solution of the Cauchy steady state heat conduction equation. *Engineering with Analysis Boundary Elements*, vol. 26, pp. 157–168.

Mitic, P.; Rashed, Y.F. (2004): Convergence and stability of the method of meshless fundamental solutions using an array of randomly distributed source. *Engineering with Analysis Boundary Elements*, vol. 28, pp. 143–153.

Morozov, V.A. (1966): On the solution of functional equations by the method of regularization, *Doklady Mathematics*, vol. 7, pp. 414–417.

Mustata, R.; Harris, S.D.; Elliott, L.; Lesnic, D.; Ingham, D.B. (2000): An inverse boundary element method for determining the hydraulic conductivity in anisotropic rocks. *CMES: Computer Modeling in Engineering & Sciences*, vol. 1, pp. 107–116.

Nardini, D.; Brebbia, C.A. (1982): A new approach to free vibration analysis using boundary elements. In: C.A. Brebbia (ed.) *Boundary Element Method in Engineering*, Springer-Verlag, Berlin, pp. 312–326.

Noroozi, S.; Sewell, P.; Vinney, J. (2006): The application of a hybrid inverse boundary element problem engine for the solution of potential problems. *CMES: Computer Modeling in Engineering & Sciences*, vol. 14, pp. 171–180.

Nowak, A.J.; Neves, A.C. (1994): Fundamentals of the multiple reciprocity method. In: A.J. Nowak & A.C. Neves (eds.) *The Multiple Reciprocity Boundary Element Methods*, WIT Press and Computational Mechanics Publications, Boston, pp. 25–43.

Partridge, P.W.; Brebbia, C.A.; Wrobel, L.C. (1992): *The Dual Reciprocity Boundary Element Method*, Computational Mechanics Publications and Elsevier, London.

Poullikkas, A.; Karageorghis, A.; Georgiou, G. (1998a): Methods of fundamental solutions for harmonic and biharmonic boundary value problems. *Computational Mechanics*, vol. 21, pp. 416–423.

Poullikkas, A.; Karageorghis, A.; Georgiou, G. (1998b): The method of fundamental solutions for inhomogeneous elliptic problems, *Computa-*

tional Mechanics, vol. 22, pp. 100–107.

Poullikkas, A.; Karageorghis, A.; Georgiou, G. (2001): The numerical solution of three-dimensional Signorini problems with the method of fundamental solutions. *Engineering with Analysis Boundary Elements*, vol. 25, pp. 221–227.

Poullikkas, A.; Karageorghis, A.; Georgiou, G. (2002): The numerical solution for three-dimensional elastostatics problems. *Computers & Structures*, vol. 80, pp. 365–370.

Ramachandran, P.A. (2002): Method of fundamental solutions: Singular value decomposition analysis, *Communications in Numerical Methods in Engineering*, vol. 18, pp. 789–801.

Shiozawa, D.; Kubo, S.; Sakagami, T.; Takagi, M. (2006): Passive electric potential CT method using piezoelectric material for identification of plural cracks. *CMES: Computer Modeling in Engineering & Sciences*, vol. 11, pp. 27–36.

Tankelevich, R.; Fairweather, G.; Karageorghis, A.; Smyrlis, Y.-S. (2006): Potential field based geometric modeling using the method of fundamental solutions. *International Journal for Numerical Methods in Engineering*, vol. 68, pp. 1257–1280.

Tikhonov, A.N.; Arsenin, V.Y. (1986): *Methods for Solving Ill-Posed Problems*, Nauka, Moscow.

Vogel, C.R. (1996): Non-convergence of the L-curve regularization parameter selection method, *Inverse Problems*, vol. 12, pp. 535–547.

Wahba, G. (1977): Practical approximate solutions to linear operator equations when the data are noisy, *SIAM Journal on Numerical Analysis*, vol. 14, pp. 651–667.

Wei, T.; Hon, Y.C.; Ling, L. (2007): Method of fundamental solutions with regularization techniques for Cauchy problems of elliptic operators. *Engineering with Analysis Boundary Elements*, vol. 31, pp. 373–385.

Zeb, A.; Elliott, L.; Ingham, D.B.; Lesnic, D. (2000): Boundary element two-dimensional solution of an inverse Stokes problem. *Engineering Analysis with Boundary Elements*, vol. 24, pp. 75–88.

Zeb, A.; Elliott, L.; Ingham, D.B.; Lesnic, D.

(2002): An inverse Stokes problem using interior pressure data. *Engineering Analysis with Boundary Elements*, vol. 26, pp. 739–745.